J. Fluid Mech. (2003), *vol.* 497, *pp.* 23–53.
DOI: 10.1017/S0022112003006554 Printed in the United Kingdom

Combustion instability due to the nonlinear interaction between sound and flame

By XUESONG WU†, MENG WANG, PARVIZ MOIN AND NORBERT PETERS

Center for Turbulence Research, Stanford University, CA 94305, USA

(Received 7 August 2002 and in revised form 26 June 2003)

It has been observed in experiments that significant levels of sound may be produced when a curved flame propagates downwards along a tube in a gravity field. In this paper, we present a mathematical description of this acoustic amplification process, which represents a simple form of combustion instability. First, based on the large-activation-energy and small-Mach-number assumptions, a general asymptotic formulation is derived, in which the nature of flame–sound coupling is brought out explicitly. This framework is then employed to study the weakly nonlinear coupling between a Darrieus–Landau (D-L) instability mode of the flame and an acoustic mode of the tube, which is the main mechanism for sound generation in the experiments. In order to provide a somewhat unified description, the linear coupling via the direct pressure effect has also been included in our analysis. A set of coupled equations which govern the evolution of the acoustic and D-L modes was derived. The solutions show that the nonlinear coupling leads to very rapid amplification of sound. After reaching an appreciable level, the sound inhibits the flame, causing the latter to flatten. The sound then saturates at an almost constant level, or continues to grow at a smaller rate owing to the pressure effect. The above theoretical predictions are in good qualitative agreement with experiments. The present study also considered the influence of weak vortical disturbances in the oncoming flow. It is shown that certain components in these perturbations may form resonant triads with the acoustic and D-L modes, thereby providing an additional coupling mechanism.

1. Introduction

Combustion instability generally refers to the sustained pressure fluctuations of an acoustic nature in a chamber where unsteady combustion takes place. Because of its adverse effect on the structure and performance of the combustion, it has been a subject of extensive research.

Combustion instability is essentially a self-excited oscillation, involving a complex interplay among unsteady heat release, the acoustic fluctuation and the vorticity field. Unsteady heat release generates sound. The latter can produce a back effect on the heat release through a number of mechanisms. In a combustor containing a shear flow, which is typical of practical combustor configurations, sound may generate (Kelvin–Helmholtz) instability waves at the inlet (via a receptivity mechanism as it is usually referred to in laminar–turbulent transition). These waves then amplify,

† Present address: Department of Mathematics, Imperial College, 180 Queens Gate, London SW7 2BZ, UK.

causing the shear layer to roll up and break down into small-scale motions, which affects heat release, thereby forming a closed feedback loop (e.g. Poinsot *et al.* 1987; Yu, Trouve & Daily 1991; Schadow & Gutmark 1992). Sound may modulate the inlet feeding rate of the fuel, causing equivalence ratio oscillations (e.g. Lieuwen & Zinn 1998). Sound may affect heat release by modulating the surface area of the flame, and by modifying burning rate directly. These last two mechanisms operate in simple combustor geometry such as a tube or duct, and will be the focus of the present study. In practical situations, several mechanisms may be operating simultaneously.

An important insight into the effect of unsteady heat release on sound amplification is provided by the Rayleigh criterion, which states that an acoustic wave will amplify if its pressure and the heat release are 'in phase', i.e. the integral of the product of the pressure and the unsteady heat release over a cycle is positive. The difficulty in applying this criterion is that unsteady heat release is often part of the solution and thus not known *a priori*. A usual remedy is to extrapolate, by using available experimental data, some empirical relations between the heat release and sound fluctuation. This then leads to a thermo-acoustic problem. Such an approach has been employed by Bloxsidge, Dowling & Langhorne (1988) to describe 'reheat buzz' (Langhorne 1988). In their work, the unsteady heat release was taken to be proportional to flow velocity at the flame front with a suitable time delay. This linear relation was subsequently extended by Dowling (1997) to include nonlinear effects in order to describe the self-excited oscillations in the system. A somewhat different model, which relates the heat release to the flame surface area, was proposed by Fleifil *et al.* (1996) and was further extended by Dowling (1999) and Ducruix, Durox & Candel (2000). Ducruix *et al.* also conducted an experimental study to check the validity of the model, and concluded that the model provides a reasonably accurate approximation for sound of relatively low frequency. Dowling (1995) formulated the semi-empirical approach in a more general setting, and discussed, *inter alia*, the effects of the mean Mach number and heat distribution.

In the semi-empirical approach, the hydrodynamic (and chemical) processes of combustion are completely by-passed. To understand the acoustic-flame coupling from first principles, we have to look into the structure of the flame as well as its associated hydrodynamic field. Fortunately, for premixed flames much knowledge about the last two aspects above has been obtained by using the powerful asymptotic approach based on the large-activation-energy assumption (Williams 1985). Clavin (1985, 1994) gives detailed reviews of the subject. This framework, as well as relevant previous results, will be used in our work. Detailed discussions will be presented in § 2.

A thorough theoretical treatment of sound–flame coupling is unrealistic at present for a practical combustor, where the flow is strongly vortical and turbulent. As a first step, it is necessary to restrict the present work to the simple case where the hydrodynamic motion is primarily due to unsteady heat release and remains laminar.

A formal formulation of acoustic-flame coupling has been given by Harten, Kapila & Matkowsky (1984) for what may be called the 'high-frequency' regime, where the acoustic time scale is comparable to the transit time of the flame, $O(d/U_L)$, while the hydrodynamics has a length scale of $O(d)$; here, d and U_L represent the flame thickness and speed, respectively. The resulting system is nonlinear and requires a major numerical attack. Harten *et al.* consider the flat-flame case in the low-frequency and small-heat-release limits, and obtained in each limit the solution which describes the effect of acoustic pressure on the flame. However, they did not consider how flame influences the sound. This inverse process was investigated by Clavin, Pelce & He

(1990), who also removed the assumption of small heat release. By closing the loop, they were able to show that the mutual interaction leads to amplification of sound, i.e. to acoustic instability. For a *flat flame*, the hydrodynamics is completely absent, and the sole coupling is through the acoustic pressure affecting the temperature or enthalpy.

For a *curved flame*, there exists an additional coupling mechanism. As was pointed out by Markstein (1970), the sound pressure modulates the flame and hence alters its surface area. This in turn leads to modulation of heat release, thereby affecting the sound itself. This mechanism was further analysed by Pelce & Rochwerger (1992) in connection with the experiments of Searby (1992), who observed that sound was generated when a curved flame was propagating downwards in a tube. The curved flame arises as a result of the well-known Darrieus–Landau (D-L) instability. In developing a mathematical model, Pelce & Rochwerger represented the curved flame by the neutrally stable D-L instability mode, (which exists due to the stabilizing effect of gravity). A constant amplitude is prescribed in calculating the growth rate of the sound. The latter was found to be proportional to the square of the amplitude of the D-L mode. Their calculation further indicates that the maximum growth rate is attained when the flame has reached the lower half of the tube. This coupling mechanism could be stronger by an order of magnitude than that via pressure–temperature considered by Clavin *et al.* (1990).

The general concern of the present paper is with the flame–acoustic coupling process that leads to large-scale combustion instability in premixed flames. Previously, each mechanism of flame–acoustic coupling was treated separately and some derivations rely on *ad hoc* assumptions which are not mathematically justified. As such, the relative role of different mechanisms is not entirely clear. In the present paper, we will derive a general asymptotic theory starting from the fundamental equations governing the chemically reacting flows. The general theory will allow us not only to unify the known coupling processes, but also to identify a new one. A specific objective of the present study is to improve the model of Pelce & Rochwerger (1992) in two somewhat related aspects, both of which are important. First, we note that, like any marginally stable mode, a neutral D-L mode must modulate in a weakly nonlinear fashion rather than stay completely neutral. According to classical weakly nonlinear theory (Stuart 1960), if the typical magnitude of the mode is ϵ, the time scale of modulation is $O(\epsilon^{-2})$, which is comparable with the time scale over which the sound amplifies. Secondly, Searby's (1992) experiments showed that the flame was evolving, and moreover that sound amplification takes place mainly as the flame evolves from a curved pattern to a flat one. Therefore, for both mathematical and physical reasons, it is necessary to take into account simultaneously the evolving nature of the flame and the back reaction of sound on the flame, which were suppressed in the theory of Pelce & Rochwerger (1992) in an *ad hoc* manner. In this paper, the nonlinear coupling and evolution of the acoustic and flame instability modes will be studied in a systematic fashion by using the general asymptotic formulation.

The rest of the paper is organized as follows. In § 2, the problem is formulated for a premixed combustion in a two-dimensional duct. The relevant asymptotic scalings are specified and the resulting asymptotic structures are highlighted. In § 3, a general formulation is given for the sound–flame interaction in what may be regarded as the 'low-frequency' regime in the sense that the acoustic time scale is much longer than the transit time of the flame. The analysis indicates that the coupling in general is strongly nonlinear; the flame drives acoustic fluctuation by inducing a jump in the longitudinal velocity, while the sound so produced modulates the flame. The analysis

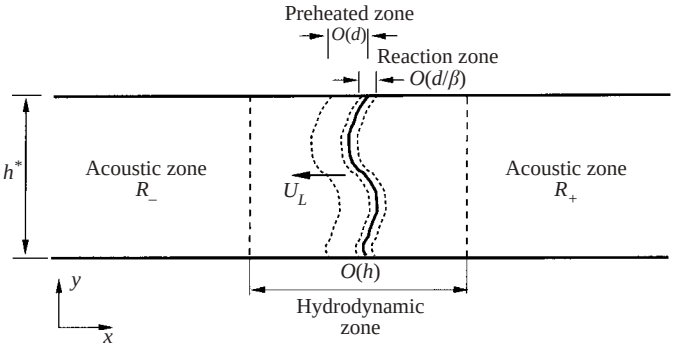

FIGURE 1. A sketch illustrating the problem and the asymptotic structure.

is extended to include the coupling mechanism due to the direct effect of pressure on the burning velocity. In § 4, the analysis is specialized to the interaction between a D-L instability mode and a longitudinal acoustic mode of the duct. With the particular purpose to explain further the experiments of Searby (1992), we assume that the flame is nearly neutral due to the stabilizing effect of gravity. A weakly nonlinear analysis is performed to derive the amplitude equations that govern the coupling between the flame and sound. The effect of vortical disturbances carried by the oncoming fresh mixture is also analysed, and we show that certain components of disturbances may form a resonant triad with the D-L and acoustic modes, thereby modifying the sound–flame coupling. Relevant numerical solutions of the amplitude equations are presented in § 5, and they indicate that the present theory captures some important features of the experiments. In § 6, we summarize the main results and discuss briefly further work.

2. Formulation

Consider the combustion of a homogeneous premixed combustible mixture in a duct of width h^* (see figure 1). For simplicity, a one-step irreversible exothermic chemical reaction is assumed. The gaseous mixture consists of a single deficient reactant and an abundant component so that the progressive variable of the reaction can be taken to be the mass fraction of the former, Y, and the physical properties are determined by the latter. The mixture is assumed to obey the state equation for a perfect gas.

The fresh mixture has a density $\rho_{-\infty}$ and temperature $\Theta_{-\infty}$. Owing to steady heat release, the mean temperature (density) behind the flame increases (decreases) to Θ_∞ (ρ_∞). An important non-dimensional parameter is

$$\beta = E(\Theta_\infty - \Theta_{-\infty})/\mathscr{R}\Theta_\infty^2, \tag{2.1}$$

where E is the activation energy and $\mathscr{R}$ is the universal gas constant.

The flame propagates into the fresh mixture at a mean speed U_L, and it has an intrinsic thickness $d = D_{th}^*/U_L$, where D_{th}^* is the thermal diffusivity. For later reference, we define the ratio

$$\delta = d/h^*,$$

and the Mach number

$$M = U_L/a^*,$$

where $a^* = (\gamma p_{-\infty}/\rho_{-\infty})^{1/2}$ is the speed of sound.

The formulation in this section follows closely that of Matalon & Matkowsky (1982), subject to some minor modifications due to the inclusion of compressibility and gravity force. Let (x, y, z) and t be space and time variables normalized by h^* and h^*/U_L, respectively. The velocity $\boldsymbol{u} \equiv (u, v, w)$, density ρ, and temperature θ are normalized by U_L, $\rho_{-\infty}$ and $\Theta_{-\infty}$, respectively. The non-dimensional pressure p is introduced by writing the dimensional pressure as $(p_{-\infty} + \rho_{-\infty} U_L^2 p)$.

On the assumptions that the shear viscosity is independent of temperature and bulk viscosity is zero (Stokes hypothesis), the governing equations in the non-dimensional form can be written as

$$\frac{\partial \rho}{\partial t} + \nabla \cdot (\rho \boldsymbol{u}) = 0, \tag{2.2}$$

$$\rho \left(\frac{\partial}{\partial t} + \boldsymbol{u} \cdot \nabla \right) \boldsymbol{u} = -\nabla p + \delta Pr \nabla^2 \boldsymbol{u} + \tfrac{1}{3} \delta Pr \nabla (\nabla \cdot \boldsymbol{u}) - \rho G \boldsymbol{i}, \tag{2.3}$$

$$\rho \left(\frac{\partial}{\partial t} + \boldsymbol{u} \cdot \nabla \right) Y = \delta Le^{-1} \nabla^2 Y - \delta \Omega, \tag{2.4}$$

$$\rho \left(\frac{\partial}{\partial t} + \boldsymbol{u} \cdot \nabla \right) \theta = \delta q \Omega + (\gamma - 1) M^2 \left(\frac{\partial}{\partial t} + \boldsymbol{u} \cdot \nabla \right) p + \delta \nabla^2 \theta + \delta (\gamma - 1) M^2 \Phi, \tag{2.5}$$

$$1 + \gamma M^2 p = \rho \theta, \tag{2.6}$$

where P_r, Le and γ denote the Prandtl number, Lewis number and the ratio of specific heats respectively, $\boldsymbol{i}$ is the unit vector along the duct and

$$G = g h^* / U_L^2$$

is the normalized gravity force. Φ is the dissipation function, which plays no part to the required order of approximation in this study and will be ignored here in after.

The reaction rate Ω is taken to be described by the Arrhenius law:

$$\Omega = \Omega_0 \delta^{-2} \rho Y \exp \left\{ \beta \left(\frac{1}{\Theta_+} - \frac{1}{\theta} \right) \right\}, \tag{2.7}$$

where $\Theta_+ = 1 + q$ is the adiabatic flame temperature, and the factor Ω_0 is chosen so that the non-dimensional speed of a flat flame is unity.

The basic governing equations (2.2)–(2.6) have to be supplemented by appropriate boundary conditions, which necessarily depend on the specific problem under consideration. Correct prescription of these conditions is crucial and very often a delicate matter itself.

Direct numerical simulation of combustion instability based on (2.2)–(2.6) is challenging owing to the disparity of the scales involved in the combustion process, which includes the chemical reaction taking place on a scale smaller than the Kolmogrov scale, and the acoustic fluctuation, whose wavelength is very long for a typical low-Mach-number flow.

The very fact that causes numerical difficulty, i.e. the scale disparity, may be exploited mathematically to derive a simplified system, which could provide useful theoretical insights into the problem. A key simplifying assumption is that of large activation energy, corresponding to $\beta \gg 1$. The chemical reaction then occurs in a thin region of width $O(d/\beta)$ centred at the flame front. The basic framework based on this observation has been well developed, and is referred to as large-activation-energy asymptotics.

Assume that the flame front is given by $x = f(y, z, t)$. It is convenient to introduce a coordinate system attached to the front,

$$\xi = x - f(y, z, t), \quad \eta = y, \quad \zeta = z,$$

and to split the velocity $\boldsymbol{u}$ as

$$\boldsymbol{u} = u\boldsymbol{i} + \boldsymbol{v}.$$

Then the governing equations can be written as (Matalon & Matkowsky 1982)

$$\frac{\partial \rho}{\partial t} + \frac{\partial \rho s}{\partial \xi} + \nabla \cdot (\rho \boldsymbol{v}) = 0, \tag{2.8}$$

$$\rho \frac{\partial u}{\partial t} + \rho s \frac{\partial u}{\partial \xi} + \rho \boldsymbol{v} \cdot \nabla u = -\frac{\partial p}{\partial \xi} + \delta Pr \left\{ \Delta u + \frac{1}{3} \frac{\partial}{\partial \xi} \left(\frac{\partial s}{\partial \xi} + \nabla \cdot \boldsymbol{v} \right) \right\} - \rho G, \tag{2.9}$$

$$\rho \frac{\partial \boldsymbol{v}}{\partial t} + \rho s \frac{\partial \boldsymbol{v}}{\partial \xi} + \rho \boldsymbol{v} \cdot \nabla \boldsymbol{v} = -\nabla p + \nabla f \frac{\partial p}{\partial \xi} + \delta Pr \left\{ \Delta \boldsymbol{v} + \frac{1}{3} \left(\nabla - \nabla f \frac{\partial}{\partial \xi} \right) \left(\frac{\partial s}{\partial \xi} + \nabla \cdot \boldsymbol{v} \right) \right\}, \tag{2.10}$$

$$\rho \frac{\partial Y}{\partial t} + \rho s \frac{\partial Y}{\partial \xi} + \rho \boldsymbol{v} \cdot \nabla Y = \delta Le^{-1} \Delta Y - \delta \Omega, \tag{2.11}$$

$$\rho \frac{\partial \theta}{\partial t} + \rho s \frac{\partial \theta}{\partial \xi} + \rho \boldsymbol{v} \cdot \nabla \theta = \delta \Delta \theta + \delta q \Omega + (\gamma - 1) M^2 \left(\frac{\partial p}{\partial t} + s \frac{\partial p}{\partial \xi} + \boldsymbol{v} \cdot \nabla p \right), \tag{2.12}$$

where

$$s = u - f_t - \boldsymbol{v} \cdot \nabla f,$$

$$\Delta = [1 + (\nabla f)^2] \frac{\partial^2}{\partial \xi^2} + \nabla^2 - \nabla^2 f \frac{\partial}{\partial \xi} - 2 \frac{\partial}{\partial \xi} (\nabla f \cdot \nabla);$$

here the operators ∇ and ∇^2 are defined with respect to η and ζ.

The large-activation-energy asymptotic approach requires the Lewis number Le to be close to unity, or more precisely

$$L_e = 1 + \beta^{-1} l \quad \text{with} \quad l = O(1). \tag{2.13}$$

To make analytical progress, we assume, in addition to $\beta \gg 1$, that

$$\delta = d/h^* \ll 1, \quad M \ll 1. \tag{2.14}$$

The whole flow field is then described by four distinct asymptotic regions, as illustrated in figure 1. In addition to the thin reaction and pre-heated zones, there are also hydrodynamic and acoustic regions, which scale on h^* and $\lambda^* \equiv h^*/M$, respectively.

In the reaction zone, the heat release due to the reaction balances the thermal diffusion, and the species variation balances the mass diffusion (Matkowsky & Sivashinsky 1979). In the pre-heated zone, the dominant balance is between the advection and diffusion. All the four regions are fully interactive in the sense that the final complete solution relies on the investigation of all these regions.

The direct interaction between the sound and flame is through the hydrodynamic region, which we now consider. In this region, the solution expands as

$$\left.\begin{aligned} &(\rho, \theta) = (R_0, \Theta) + \delta(\rho_1, \theta_1) + \ldots, \\ &(u, \boldsymbol{v}, f) = (u_0, \boldsymbol{v}_0, f_0) + \delta(u_1, \boldsymbol{v}_1, f_1) + \ldots, \\ &p = -(R_0 G \xi) + p_0 + \delta p_1 + \ldots. \end{aligned}\right\} \tag{2.15}$$

The solution for the mean density (Matalon & Matkowsky 1982; Pelce & Clavin 1982)

$$R_0 = \begin{cases} 1 \equiv R_-, & \xi < 0, \\ (1+q)^{-1} \equiv R_+, & \xi > 0, \end{cases}$$

is accurate to all orders in δ. In the following, the subscript '0' will be omitted. Substitution of (2.15) into (2.8)–(2.10) leads to the equations governing $(u_0, \boldsymbol{v}_0, p_0)$:

$$\left.\begin{aligned} &\frac{\partial s_0}{\partial \xi} + \nabla \cdot \boldsymbol{v}_0 = 0, \\ &R\left\{\frac{\partial u_0}{\partial t} + s_0 \frac{\partial u_0}{\partial \xi} + \boldsymbol{v}_0 \cdot \nabla u_0\right\} = -\frac{\partial p_0}{\partial \xi}, \\ &R\left\{\frac{\partial \boldsymbol{v}_0}{\partial t} + s_0 \frac{\partial \boldsymbol{v}_0}{\partial \xi} + \boldsymbol{v}_0 \cdot \nabla \boldsymbol{v}_0\right\} = -\nabla p_0 + \nabla f_0 \frac{\partial p_0}{\partial \xi} - RG\nabla f_0, \end{aligned}\right\} \tag{2.16}$$

where

$$s_0 = u_0 - f_{0,t} - \boldsymbol{v}_0 \cdot \nabla f_0. \tag{2.17}$$

Embedded in the hydrodynamic zone is the pre-heated zone, which in turn contains the much thinner reaction zone. The jump conditions across the pre-heated zone were first derived by Pelce & Clavin (1982) for $\boldsymbol{v}$, $f \ll O(1)$, and by Matalon & Matkowsky (1982) in the general case where $\boldsymbol{v}$, $f \sim O(1)$. These are

$$[u_0] = q[1 + (\nabla f_0)^2]^{-1/2}, \quad [\boldsymbol{v}_0] = -q\nabla f_0/[1 + (\nabla f_0)^2]^{1/2}, \quad [p_0] = -q. \tag{2.18}$$

The front evolution is governed by the equation

$$f_{0,t} = u_0(0^-, \eta, \zeta, t) - \boldsymbol{v}_0(0^-, \eta, \zeta, t) \cdot \nabla f_0 - [1 + (\nabla f_0)^2]^{1/2}. \tag{2.19}$$

The results (2.18)–(2.19) were originally derived by assuming that the flow is incompressible, and also by using the jump conditions across the reaction sheet. Fortunately, they are valid for small-Mach-number flows because the acoustic pressure does not affect directly the pre-heated or the reaction zone to leading-order. It only contributes a small correction at a higher order (cf. Clavin *et al.* 1990). We shall consider this effect in § 3.3.

The leading-order system (2.16)–(2.19) suffices for the most part of our work. However, a more general result may be derived if the $O(\delta)$ correction is included. The jumps at this order were obtained by Pelce & Clavin (1982) under linear approximation, and by Matalon & Matkowsky (1982) for the nonlinear case but without gravity. We repeated the analysis of the latter authors with gravity included, and found that gravity only affected the jump in $\boldsymbol{v}_1$. For later application, these $O(\delta)$ jumps are listed below:

$$\begin{aligned} [u_1] = &-\frac{lq\,D(q)}{2m_0^2}\left\{\nabla^2 f_0 + m_0 \nabla \cdot \boldsymbol{v}_0 + \frac{\mathrm{D}m_0}{\mathrm{D}t}\right\} - \frac{q}{m_0^3}\nabla f_0 \cdot \nabla f_1 \\ &+ \chi m_0\left\{\left[\frac{\partial \boldsymbol{v}_0}{\partial \xi} \cdot \nabla f_0\right] + q\nabla \cdot \frac{\nabla f_0}{m_0} - \frac{q}{m_0^3}\nabla^2 f_0 + \frac{2q}{m_0^4}\nabla m_0 \cdot \nabla f_0\right\}, \end{aligned} \tag{2.20}$$

$$\begin{aligned} [\boldsymbol{v}_1] = \chi\left\{\frac{q}{1+q}\left\{\frac{\tilde{\mathrm{D}}\boldsymbol{v}_0}{\tilde{\mathrm{D}}t} + \nabla f_0 \frac{\tilde{\mathrm{D}}u_0}{\tilde{\mathrm{D}}t} + \frac{1}{m_0}\frac{\tilde{\mathrm{D}}}{\tilde{\mathrm{D}}t}\nabla f_0 + G\nabla f_0\right\} - \frac{q}{m_0}\nabla m_0\right\} \\ - [u_1]\nabla f_0 - \frac{q}{m_0}(\nabla f_1 - \chi \nabla m_0), \end{aligned} \tag{2.21}$$

$$[p_1] = -2m_0[u_1] + (Pr+\chi)m_0^2\left\{\left[\frac{\partial \boldsymbol{v}_0}{\partial \xi}\cdot\nabla f_0\right] + q\nabla\cdot\frac{\nabla f_0}{m_0} - \frac{q}{m_0^3}\nabla^2 f_0 + \frac{2q}{m_0^4}\nabla m_0\cdot\nabla f_0\right\}$$
$$+ \frac{q}{m_0}\nabla^2 f_0 - \frac{2q}{m_0^2}\nabla f_0\cdot\nabla f_1 - \frac{q}{m_0^2}\nabla f_0\cdot\nabla m_0$$
$$+ \ln(1+q)\left\{m_0\frac{\mathrm{D}u_0}{\mathrm{D}t} + \frac{1}{m_0}\frac{\mathrm{D}m_0}{\mathrm{D}t} + \nabla f_0\cdot\left(\nabla u_0 + \frac{1}{m_0^2}\nabla m_0\right)\right\}, \tag{2.22}$$

where u_0 and $\boldsymbol{v}_0$ and their derivatives are evaluated at the front $\xi = 0^-$, and

$$m_0 = [1+(\nabla f_0)^2]^{1/2}, \quad D(q) = \int_0^\infty \ln(1+q\,\mathrm{e}^{-x})\,\mathrm{d}x, \quad \chi = Pr + \frac{1+q}{q}\ln(1+q),$$
$$\frac{\mathrm{D}}{\mathrm{D}t} = \frac{\partial}{\partial t} + \boldsymbol{v}_0(0^-,\eta,\zeta)\cdot\nabla, \quad \frac{\tilde{\mathrm{D}}}{\tilde{\mathrm{D}}t} = \frac{\mathrm{D}}{\mathrm{D}t} + \frac{\nabla f_0\cdot\nabla}{m_0}.$$

The function f_1 satisfies the equation

$$f_{1,t} = u_1(0^-,\eta,\zeta,t) - \boldsymbol{v}_0(0^-,\eta,\zeta,t)\cdot\nabla f_1 - \boldsymbol{v}_1(0^-,\eta,\zeta,t)\cdot\nabla f_0 - \frac{1}{m_0}\nabla f_0\cdot\nabla f_1$$
$$+ \left\{\frac{1+q}{q}\ln(1+q) + \tfrac{1}{2}lD(q)\right\}\left\{\nabla^2 f_0 + m_0\nabla\cdot\boldsymbol{v}_0 + \frac{\mathrm{D}m_0}{\mathrm{D}t}\right\}. \tag{2.23}$$

3. Strongly nonlinear sound–flame interaction: a general formulation

3.1. *Acoustic zone*

The appropriate variable describing the acoustic motion in this region is

$$\tilde{\xi} = M\xi. \tag{3.1}$$

Because the transverse length is much smaller than the longitudinal length, the motion is a longitudinal oscillation about the uniform mean background, and the solution can be written as

$$u = U_\pm + u_a(\tilde{\xi},t) + \ldots, \quad p = M^{-1}p_a(\tilde{\xi},t) + \ldots, \tag{3.2}$$
$$\rho = R + M\rho_a(\tilde{\xi},t) + \ldots, \quad \theta = \Theta + M\theta_a(\tilde{\xi},t) + \ldots, \tag{3.3}$$

where $U_\pm$ are the mean velocities behind and in front of the flame, respectively, with $U_+ - U_- = q$. The unsteady field is governed by the linearized equations

$$\frac{\partial \rho_a}{\partial t} + R\frac{\partial u_a}{\partial \tilde{\xi}} = 0, \quad R\frac{\partial u_a}{\partial t} = -\frac{\partial p_a}{\partial \tilde{\xi}}, \tag{3.4}$$
$$R\frac{\partial \theta_a}{\partial t} = (\gamma-1)\frac{\partial p_a}{\partial t}, \quad \gamma p_a = R\theta_a + \Theta\rho_a. \tag{3.5}$$

Elimination of θ_a and ρ_a among the above equations yields the wave equation for the pressure p_a

$$R\frac{\partial^2 p_a}{\partial t^2} - \frac{\partial^2 p_a}{\partial \tilde{\xi}^2} = 0, \quad R\frac{\partial u_a}{\partial t} = -\frac{\partial p_a}{\partial \tilde{\xi}}. \tag{3.6}$$

As $\tilde{\xi} \to \pm 0$,

$$u_a \to u_a(0^\pm,t) + \ldots, \quad p_a \to p_a(0,t) + p_{a,\tilde{\xi}}(0^\pm,t)\tilde{\xi} + \ldots.$$

As will be shown in § 3.2, the acoustic pressure is continuous across the flame, but the flame induces a jump in u_a, i.e.

$$[p_a] = 0, \quad [u_a] = q\{\overline{(1+(\nabla F_0)^2)^{1/2}} - 1\}, \tag{3.7}$$

where $\overline{\phi}$ stands for the space average of ϕ in the (η, ζ)-plane, and F_0 is defined in (3.8) below. Obviously, the jump $[u_a]$ acts as an acoustic source.

3.2. *Hydrodynamic region*

In the hydrodynamics region, u_a and $p_{a,\tilde{\xi}}$ appear spatially uniform on either side of the flame, and can be approximated by their values at $\tilde{\xi} = 0^{\pm}$. In order to facilitate the matching with the solution in the acoustic region, we subtract from the total field the acoustic components as well as the mean background flow by writing

$$\left.\begin{aligned} u_0 &= U_{\pm} + u_a(0^{\pm}, t) + U_0, \\ p_0 &= \frac{1}{M} p_a(0,t) + P_{\pm} + p_{a,\tilde{\xi}}(0^{\pm}, t)\xi + (p_{a,\tilde{\xi}}(0^{\pm}, t) - RG)F_0 + P_0, \\ f_0 &= F_a + F_0, \end{aligned}\right\} \tag{3.8}$$

where $P_{\pm}$ is the mean pressure (with $P_+ - P_- = q$), and

$$F_a' = U_- - 1 + u_a(0^-, t).$$

Let $\boldsymbol{v}_0 = \boldsymbol{V}_0$. Then it follows from (2.16)–(2.19) that the leading-order hydrodynamic field satisfies the following equations

$$\frac{\partial U_0}{\partial \xi} + \nabla \cdot \boldsymbol{V}_0 = \frac{\partial \boldsymbol{V}_0}{\partial \xi} \cdot \nabla F_0, \tag{3.9}$$

$$\frac{\partial U_0}{\partial \xi} + R\left\{\frac{\partial U_0}{\partial t} + S_0 \frac{\partial U_0}{\partial \xi} + \boldsymbol{V}_0 \cdot \nabla U_0\right\} = -\frac{\partial P_0}{\partial \xi} - R\mathscr{J} h(\xi) \frac{\partial U_0}{\partial \xi}, \tag{3.10}$$

$$\frac{\partial \boldsymbol{V}_0}{\partial \xi} + R\left\{\frac{\partial \boldsymbol{V}_0}{\partial t} + S_0 \frac{\partial \boldsymbol{V}_0}{\partial \xi} + \boldsymbol{V}_0 \cdot \nabla \boldsymbol{V}_0\right\} = -\nabla P_0 + \nabla F_0 \frac{\partial P_0}{\partial \xi} - R\mathscr{J} h(\xi) \frac{\partial \boldsymbol{V}_0}{\partial \xi}, \tag{3.11}$$

while the flame front is governed by

$$F_{0,t} = U_0(0^-, \eta, \zeta) - \boldsymbol{V}_0(0^-, \eta, \zeta) \cdot \nabla F_0 - \{(1+(\nabla F_0)^2)^{1/2} - 1\}, \tag{3.12}$$

where $h(\xi)$ is the Heaviside step function, and

$$\mathscr{J} = [u_a], \quad S_0 = U_0 - F_{0,t} - \boldsymbol{V}_0 \cdot \nabla F_0. \tag{3.13}$$

If no vortical fluctuation is present in the oncoming flow, then matching with the outer acoustic solution requires that

$$U_0 \to 0, \quad \boldsymbol{V}_0 \to 0, \quad P_{0,\xi} \to 0 \quad \text{as} \quad \xi \to \pm\infty. \tag{3.14}$$

However, non-zero far-field conditions must be imposed if the oncoming flow carries vortical disturbances.

The unsteady pressure and transverse velocity jumps are

$$\left.\begin{aligned} [P_0] &= [(R_+ - R_-)G - (p_{a,\tilde{\xi}}(0^+, t) - p_{a,\tilde{\xi}}(0^-, t))]F_0, \\ [\boldsymbol{V}_0] &= -q\nabla F_0 / [1 + (\nabla F_0)^2]^{1/2}. \end{aligned}\right\} \tag{3.15}$$

The first relation implies that the effect of sound on the flame is somewhat analogous to that of gravity, i.e. it generates the effective acceleration.

The hydrodynamic motion affects the ambient acoustic regions by inducing a longitudinal velocity jump. To derive this key result, we take the spatial average of (3.9) in the (η, ζ)-plane, and then integrate with respect to ξ to obtain

$$\overline{U_0} = \overline{\boldsymbol{V}_0 \cdot \nabla F_0}, \tag{3.16}$$

where the overbar denotes the mentioned spatial average. Inserting the first equation in (3.8) into (2.18) and taking the spatial average of the first jump relation in (2.18), we find

$$[u_a] = -[\overline{\boldsymbol{V}_0 \cdot \nabla F_0}] + q\{\overline{(1 + (\nabla F_0)^2)^{-1/2}} - 1\}$$

which, by virtue of the second relation in (3.15), simplifies to

$$\mathscr{J} = [u_a] = q\{\overline{(1 + (\nabla F_0)^2)^{1/2}} - 1\}. \tag{3.17}$$

On the scale of acoustic wavelength, the right-hand side of the above is equivalent to a concentrated unsteady heat release rate, which is shown to be proportional to the increase of the flame surface area. Result (3.17) is of fundamental significance. It implies that a curved flame evolving on the acoustic time scale of the duct must generate sound, that is, acoustic field is an integral part of the flame. We are not aware of a previous mathematical derivation of this relation, though it has been employed on the physical ground by Pelce & Rochwerger (1992), Fleifil *et al.* (1996) and Ducruix *et al.* (2000) to formulate their flame–acoustic coupling theories.

The jump condition across the flame for U_0 becomes

$$[U_0] = q\{(1 + (\nabla F_0)^2)^{-1/2} - \overline{(1 + (\nabla F_0)^2)^{1/2}}\}. \tag{3.18}$$

The hydrodynamic equations (3.9)–(3.12) and the acoustic equations (3.6) form an overall interactive system via the jump conditions (3.7) and (3.15). The nature of the interaction between the flame and sound is explicit: the flame generates sound through the change of its surface area, while sound modulates the flame by producing an effective acceleration.

The asymptotically reduced system uses two distinct spatial variables to describe two distinct motions so that, in terms of $\tilde{\xi}$, the acoustic motion has an $O(1)$ characteristic speed (see (3.6)), comparable with the hydrodynamic velocity. This has a significant advantage from the numerical point of view, because the sound speed now does not impose a severe restriction on the time step. The reduced system thus avoids the major difficulty associated with the numerical approximation of the original system.

3.3. *Coupling via the direct effect of pressure on the burning velocity*

In §§ 3.1 and 3.2, the acoustic pressure is shown to modulate the hydrodynamic field associated with the flame, thereby affecting the flame motion. An additional effect of pressure is to influence the enthalpy balance, thereby modifying the burning velocity. Acoustic–flame coupling through this mechanism will be considered in this subsection.

The effect of external pressure variations on premixed flames was analysed by Peters & Ludford (1984) for a one-dimensional flame and by Keller & Peters (1994) for a general three-dimensional flame. Both investigations were concerned with a slowly varying pressure in the sense that the time scale is much larger than $O(d/U_L)$, the transit time scale. McIntosh (1991, 1993) and McIntosh & Wilce (1991) demonstrated that several distinct regimes emerge depending on the characteristic time scales of the pressure fluctuation. They analysed in detail the response of the burning rate in each regime for a one-dimensional flame.

An important observation is that a small-amplitude pressure variation of $O(\beta^{-1})$ may exert an order-one effect on the flame speed. In our problem, the acoustic

pressure, that is generated owing to the change in the flame surface area, is of $O(M)$, and thus it will produce an $O(\beta M)$ modification to the flame burning velocity. To analyse this effect, it is convenient to work with the enthalpy h, defined as

$$\theta + qY = 1 + q + \beta^{-1}h.$$

In the hydrodynamic region, h expands as

$$h = \beta M\tilde{H} + \ldots,$$

and $\tilde{H}$ satisfies

$$\frac{\partial \tilde{H}}{\partial \xi} + R\left\{\frac{\partial \tilde{H}}{\partial t} + S_0\frac{\partial \tilde{H}}{\partial \xi} + \boldsymbol{V}_0\cdot\nabla\tilde{H}\right\} = (\gamma-1)\frac{\partial p_a}{\partial t} - R\mathscr{J}h(\xi)\frac{\partial \tilde{H}}{\partial \xi}.$$

Assuming that there is no enthalpy fluctuation present in the upstream, we have for $\xi < 0$,

$$\tilde{H} = R_-^{-1}(\gamma-1)p_a(0,t) \equiv \theta_a(0^-,t).$$

The above expression, however, does not satisfy the equation for $\xi > 0$, where the solution may be written as

$$\tilde{H} = R_+^{-1}(\gamma-1)p_a(0,t) + \tilde{H}_e$$

with $\tilde{H}_e$ satisfying the equation

$$\frac{\partial \tilde{H}_e}{\partial \xi} + R_+\left\{\frac{\partial \tilde{H}_e}{\partial t} + S_0\frac{\partial \tilde{H}_e}{\partial \xi} + \boldsymbol{V}_0\cdot\nabla\tilde{H}_e\right\} = -R_+\mathscr{J}\frac{\partial \tilde{H}_e}{\partial \xi},$$

and the boundary condition

$$\tilde{H}_e \to -q(\gamma-1)p_a(0,t) \quad \text{as} \quad \xi \to 0.$$

The relevant solution is independent of η and ζ, and can be written in an implicit form using characteristics. We shall omit it since it is not needed for the subsequent analysis. Nevertheless, it is worth noting that $\tilde{H}_e$ represents the enthalpy motion downstream of the flame front that is generated by the acoustic pressure. This interpretation is best illustrated by noting that in the linear limit,

$$\tilde{H}_e = -q(\gamma-1)p_a(0, t-\xi/(1+q)),$$

which corresponds to the reactant mass fraction $\tilde{Y} = -(\gamma-1)p_a(0, t-\xi/(1+q))$, implying that unburned material is advected downstream.

To take account of the $O(\beta M)$ effect, the expansion for u, $\boldsymbol{v}$, p and f must be extended to

$$(u, \boldsymbol{v}, p, f) = (u_0, \boldsymbol{v}_0, p_0, f_0) + \delta(u_1, \boldsymbol{v}_1, p_1, f_1) + \beta M(\tilde{U}, \tilde{\boldsymbol{V}}, \tilde{P}, \tilde{f}) + \ldots.$$

In order to derive the jumps in $\tilde{U}$, $\tilde{\boldsymbol{V}}$ and $\tilde{P}$, we must consider the pre-heated zone.

According to the discussion in § 1, the appropriate longitudinal variable describing the the pre-heated zone is $\hat{\xi} = \xi/\delta$. The expansion takes the form

$$\begin{aligned}
h &= h_0 + \delta h_1 + \beta M\tilde{h} + \ldots,\\
\theta &= \theta_0 + \delta\theta_1 + \beta M\tilde{\theta} + \ldots,\\
m &= m_0 + \delta m_1 + \beta M\tilde{m} + \ldots,\\
u &= u_0 + \delta u_1 + \beta M\tilde{u} + \ldots,\\
\boldsymbol{v} &= \boldsymbol{v}_0 + \delta\boldsymbol{v}_1 + \beta M\tilde{\boldsymbol{v}} + \ldots,
\end{aligned}$$

where $m = \rho s$. The solutions at the first two orders are given by Matalon & Matkowsky (1982), and in particular

$$\theta_0 = 1 + q\,\mathrm{e}^{\hat{\xi}/m_0}, \quad h_0 = -\frac{ql}{m_0}\hat{\xi}\,\mathrm{e}^{\hat{\xi}/m_0}.$$

Let us now consider $\tilde{h}$ and $\tilde{\theta}$. They are governed by the equations

$$\left.\begin{aligned} m_0\frac{\partial\tilde{\theta}}{\partial\hat{\xi}} - m_0^2\frac{\partial^2\tilde{\theta}}{\partial\hat{\xi}^2} &= -\tilde{m}\frac{\partial\theta_0}{\partial\hat{\xi}} + 2\nabla f_0\cdot\nabla\tilde{f}\frac{\partial^2\theta_0}{\partial\hat{\xi}^2}, \\ m_0\frac{\partial\tilde{h}}{\partial\hat{\xi}} - m_0^2\frac{\partial^2\tilde{h}}{\partial\hat{\xi}^2} &= -\tilde{m}\frac{\partial\theta_0}{\partial\hat{\xi}} + lm_0^2\frac{\partial^2\tilde{h}}{\partial\hat{\xi}^2} + 2\nabla f_0\cdot\nabla\tilde{f}\left[l\frac{\partial^2\theta_0}{\partial\hat{\xi}^2} + \frac{\partial^2 h_0}{\partial\hat{\xi}^2}\right]. \end{aligned}\right\} \tag{3.19}$$

Note that the acoustic pressure does not appear in the equations. Across the reaction sheet at $\hat{\xi} = 0$, the following jump conditions hold (Matkowsky & Sivashinsky 1979)

$$[\tilde{h}] = [\tilde{\theta}] = 0, \quad \left[l\frac{\partial\tilde{\theta}}{\partial\hat{\xi}} + \frac{\partial\tilde{h}}{\partial\hat{\xi}}\right] = 0, \quad m_0\left[\frac{\partial\tilde{\theta}}{\partial\hat{\xi}}\right] = -\tfrac{1}{2}q\tilde{h}(0) + \frac{q}{m_0^2}\nabla f_0\cdot\nabla\tilde{f}.$$

For $\hat{\xi} > 0$, the right-hand sides of (3.19) are identically zero, implying that $\tilde{\theta} = 0$ and $\tilde{h} = \tilde{h}(\eta, \zeta, t)$. For $\hat{\xi} < 0$, the solution is found to be

$$\tilde{\theta} = \frac{q}{m_0^2}\left(\tilde{m} - \frac{2}{m_0}\nabla f_0\cdot\nabla\tilde{f}\right)\hat{\xi}\exp(\hat{\xi}/m_0),$$

$$\tilde{h} = \tilde{h}_{-\infty} - l\left\{\frac{q}{m_0^2}\left(\tilde{m} - \frac{2}{m_0}\nabla f_0\cdot\nabla\tilde{f}\right) + \frac{q}{m_0^3}\left(\tilde{m} - \frac{2}{m_0}\nabla f_0\cdot\nabla\tilde{f}\right)\hat{\xi}\right\}\hat{\xi}\exp(\hat{\xi}/m_0),$$

$$\tilde{m} = \tfrac{1}{2}m_0\tilde{h}_{-\infty} + \frac{1}{m_0}\nabla f_0\cdot\nabla\tilde{f}.$$

Matching with the solution in the upstream hydrodynamic zone yields

$$h_{-\infty} = \tilde{H}(0, t) = (\gamma - 1)p_a(0, t).$$

Note that the acoustic pressure affects the flame speed by modifying the enthalpy upstream of the flame zone, rather than by acting on the enthalpy in the flame zone directly. The latter process produces a much smaller effect of $O(\delta\beta M)$ (cf. Keller & Peters 1994). If the flame is taken to be flat, the present result reduces to the low-frequency limit of Clavin *et al.* (1990) and McIntosh (1991). It is also consistent with that of Harten *et al.* (1984) if allowance is given to the difference in the assumed pressure amplitudes.

Consideration of $\tilde{u}$ and $\tilde{\boldsymbol{v}}$ determines the jumps across the flame zone for the velocity and pressure in the hydrodynamic region,

$$\left.\begin{aligned} [\tilde{U}] &= \frac{q}{m_0}\left(\tfrac{1}{2}\tilde{h}_{-\infty} - \frac{1}{m_0^2}\nabla f_0\cdot\nabla\tilde{f}\right), \\ [\tilde{\boldsymbol{V}}] &= -\frac{q}{m_0}\left\{\nabla\tilde{f} + \left(\tfrac{1}{2}h_{-\infty} - \frac{\nabla f_0\cdot\nabla\tilde{f}}{m_0^2}\right)\nabla f_0\right\}, \quad [\tilde{P}] = -qh_{-\infty}, \end{aligned}\right\} \tag{3.20}$$

while the front equation is found to be

$$\tilde{f}_t + \boldsymbol{V}_0\cdot\nabla\tilde{f} + \tilde{\boldsymbol{V}}\cdot\nabla f_0 = \tilde{U}(0^-, \eta, \zeta) - \frac{1}{m_0}\nabla F_0\cdot\nabla\tilde{f} - \tfrac{1}{2}m_0\tilde{h}_{-\infty}.$$

These relations imply that enthalpy in general would induce vortical hydrodynamic motion.

To see how the $O(\beta M)$ hydrodynamic field is coupled to the acoustic field, we note that expanding the continuity equation to $O(\beta M)$ gives

$$\frac{\partial \tilde{U}}{\partial \xi} + \nabla \cdot \tilde{\boldsymbol{V}} = \frac{\partial \boldsymbol{V}_0}{\partial \xi} \cdot \nabla \tilde{f} + \frac{\partial \tilde{\boldsymbol{V}}}{\partial \xi} \cdot \nabla F_0. \tag{3.21}$$

Taking the average of this equation in the (η, ζ)-plane, and integrating from $-\infty$ to ∞, we obtain

$$[\tilde{u}_a] - [\overline{\tilde{U}}] = -\overline{[\boldsymbol{V}_0] \cdot \nabla \tilde{f}} - \overline{[\tilde{\boldsymbol{V}}] \cdot \nabla F_0} = q \overline{\left(\frac{1}{m_0} + \frac{1}{m_0^3} \right) \nabla F_0 \cdot \nabla \tilde{f}} + \tfrac{1}{2} q h_{-\infty} \frac{\overline{(\nabla F_0)^2}}{m_0}. \tag{3.22}$$

Equation (3.20) is then spatially averaged, and combined with (3.22) to give $[\tilde{u}_a]$. This $O(\beta M)$ acoustic jump is added to (3.7), leading to

$$[u_a] = q \{ \overline{(1 + (\nabla F_0)^2)^{1/2}} - 1 \} + \beta M q \left\{ \tfrac{1}{2} h_{-\infty} \overline{[1 + (\nabla F_0)^2]^{1/2}} + \frac{\overline{\nabla F_0 \cdot \nabla \tilde{f}}}{m_0} \right\}, \tag{3.23}$$

which is a generalization of (3.7). Clearly, for strongly wrinkled flames (i.e. $\nabla F_0 \sim O(1)$), the change of flame surface area, is the dominant mechanism for sound generation. For weakly wrinkled flames for which $\nabla F_0 \sim (\beta M)^{1/2}$, the two terms are formally comparable.

4. A weakly nonlinear case

A flat flame may become unstable owing to differential diffusivity of mass and heat, or to the hydrodynamic effect associated with gas expansion. The latter is the D-L instability mentioned in § 1. An interesting and important question is: how large-scale combustion instability is related to flame instabilities, which occur over small scales over which the unsteady flow can be treated as incompressible. A natural proposal is that combustion instability arises when acoustic modes of the chamber are excited and amplified by the flame instabilities through mutual resonance. D-L instability perhaps is the most important candidate for driving combustion instability since, for most mixtures, the Lewis number is close to unity so that the instability due to differential diffusivity is ruled out.

In general, D-L instability occurs at all wavenumbers and its growth rate is proportional to the wavenumber. However, it can be stabilized by the gravity effect, which introduces a small wavenumber cutoff (Pelce & Clavin 1982). The mode with this cutoff wavenumber is nearly neutral. On the other hand, an acoustic mode is neutral on the linear basis. A nonlinear interaction can take place between the two even when their respective magnitudes are still small. Such a weakly nonlinear effect can be analysed by using the general formulation in § 3, as will be shown in this section. The present analysis is motivated by the experiments of Searby (1992), where such a weakly nonlinear coupling apparently operates.

4.1. *Analysis of the hydrodynamics of the flame*

For simplicity, we assume that the flame is two dimensional. The flame is stable when the flame speed U_L is less than the critical value

$$U_c \equiv \left(\frac{g h^*}{\pi (1 + q)} \right)^{1/2}, \tag{4.1}$$

as was shown by Pelce & Clavin (1982); see also below. A D-L mode with wavenumber $k=\pi$ is nearly neutral when U_L is close to U_c. Suppose that the magnitude of such a mode is of $O(\epsilon)$. Then the weakly nonlinear interaction takes place over the time scale of $O(\epsilon^{-2})$ (Stuart 1960), and thus we introduce the slow variable

$$\tau = \epsilon^2 t. \tag{4.2}$$

In keeping with this, U_L is assumed to deviate from its critical value U_c by $O(\epsilon^2)$, and thus we write

$$\frac{gh^*}{U_L^2} = \pi(1+q) + \epsilon^2 g_d \equiv G_c + \epsilon^2 g_d \quad \text{with} \quad g_d = O(1). \tag{4.3}$$

To take into account the $O(\delta)$ effect of the Markstein length, which is associated with the diffusion structure of the flame, we assume that

$$\delta = O(\epsilon^2),$$

and without losing generality we take $\epsilon^2 = \delta$. We shall further assume that

$$\epsilon \sim (\beta M)^{1/2}$$

so as to include the direct pressure effect on the sound amplification.

The velocity and pressure in the hydrodynamic region expand as

$$(U_0, V_0, P_0) = \epsilon(\hat{U}_1, \hat{V}_1, \hat{P}_1) + \epsilon^2(\hat{U}_2, \hat{V}_2, \hat{P}_2) + \epsilon^3(\hat{U}_3, \hat{V}_3, \hat{P}_3) + \ldots. \tag{4.4}$$

The expansion of F_0 is somewhat unusual and has the form

$$F_0 = \hat{F}_0(\tau) + \epsilon \hat{F}_1 + \epsilon^2 \hat{F}_2 + \epsilon^3 \hat{F}_3 + \ldots, \tag{4.5}$$

where the $O(1)$ term is due to the accumulated effect of stretching and advection.

Substituting the expansion into (3.9)–(3.12) and expanding to $O(\epsilon^3)$, we obtain a sequence of equations at $O(\epsilon^n)$ $(n=1, 2, 3)$. The leading-order solution was given by (cf. Pelce & Clavin 1982)

$$\left.\begin{aligned} &(\hat{U}_1, \hat{P}_1, \hat{F}_1) = A(\tau)\{(-P^{\pm}\,\mathrm{e}^{\mp k\xi} + C^{\pm}),\, P^{\pm}\,\mathrm{e}^{\mp k\xi},\, F_1\}(\mathrm{e}^{\mathrm{i}k\eta} + \text{c.c.}),\\ &\hat{V}_1 = \pm A(\tau) P^{\pm}\,\mathrm{e}^{\mp k\xi}(\mathrm{i}\,\mathrm{e}^{\mathrm{i}k\eta} + \text{c.c.}), \end{aligned}\right\} \tag{4.6}$$

where A is the amplitude function of the D-L mode and is real, $C^- = 0$ to satisfy the zero velocity fluctuation condition upstream. The wavenumber $k=\pi$ so that the boundary condition, $\hat{V}_1 = 0$ at $\eta = 0, 1$, is satisfied. The front equation implies that $P^- = 0$. The jump conditions are the linearized version of (3.15) and (3.18), i.e.

$$P^+ = (R_+ - R_-)G_c F_1, \quad -P^+ + C^+ = 0, \quad P^+ = -qkF_1.$$

The requirement of a non-zero solution gives the leading-order eigen-relation (4.1). The eigenfunction is normalized by setting $F_1 = 1$, and then

$$P^+ = C^+ = -q\pi \equiv P.$$

We may be concerned with the fact that $\hat{U}_1$ does not decay to zero as $\xi \to \infty$. This seemingly worrying issue is resolved in Appendix B, where we show that decay occurs in a thicker 'buffer layer'.

To proceed to higher orders, we need to know $p_{a,\xi}(0^{\pm}, t)$, and according to the later analysis in § 4.2,

$$p_{a,\tilde{\xi}}(0^{\pm}, t) = -\epsilon R_{\pm}(\mathrm{i}\omega B \hat{u}_{a,1}\,\mathrm{e}^{\mathrm{i}\omega t} + \text{c.c.}) \equiv -\epsilon R_{\pm}\tilde{u}'_{a,1}(0, t).$$

The $O(\epsilon^2)$ terms in (4.4) and (4.5) are governed by the following system of equations

$$\frac{\partial \hat{U}_2}{\partial \xi} + \frac{\partial \hat{V}_2}{\partial \eta} = \frac{\partial \hat{V}_1}{\partial \xi}\frac{\partial \hat{F}_1}{\partial \eta}, \tag{4.7}$$

$$R\frac{\partial \hat{U}_2}{\partial t} + \frac{\partial \hat{U}_2}{\partial \xi} = -\frac{\partial \hat{P}_2}{\partial \xi} - R\left\{\hat{U}_1\frac{\partial \hat{U}_1}{\partial \xi} + \hat{V}_1\frac{\partial \hat{U}_1}{\partial \eta}\right\}, \tag{4.8}$$

$$R\frac{\partial \hat{V}_2}{\partial t} + \frac{\partial \hat{V}_2}{\partial \xi} = -\frac{\partial \hat{P}_2}{\partial \eta} - R\left\{\hat{U}_1\frac{\partial \hat{V}_1}{\partial \xi} + \hat{V}_1\frac{\partial \hat{V}_1}{\partial \eta}\right\} + \frac{\partial \hat{P}_1}{\partial \xi}\frac{\partial \hat{F}_1}{\partial \eta}, \tag{4.9}$$

$$\hat{F}_{0,\tau} + \hat{F}_{2,t} = \hat{U}_2(0^-, \eta, t) - \hat{V}_1(0^-, \eta, t)\frac{\partial \hat{F}_1}{\partial \eta} - \frac{1}{2}\left(\frac{\partial \hat{F}_1}{\partial \eta}\right)^2. \tag{4.10}$$

The jumps follow from the expansion of (3.15) and (3.18), which shows that at $O(\epsilon^2)$,

$$\left.\begin{aligned} [\hat{U}_2] &= -\tfrac{1}{2}q[(\nabla \hat{F}_1)^2 + \overline{(\nabla \hat{F}_1)^2}], \\ [\hat{V}_2] &= -q\nabla \hat{F}_2, \\ [\hat{P}_2] &= (R_+ - R_-)(G_c\hat{F}_2 + \tilde{u}'_{a,1}(0,t)\hat{F}_1), \end{aligned}\right\} \tag{4.11}$$

As the forcing terms on the right-hand side indicate, there exists a mutual interaction between the sound and flame as well as the self-interaction of the flame. Inspection of the forcing terms suggest that the solution takes the form

$$\left.\begin{aligned} \hat{U}_2 &= \hat{U}_{2,a}(\mathrm{e}^{\mathrm{i}k\eta} + \text{c.c.})\,\mathrm{e}^{\mathrm{i}\omega t} + \text{c.c.} + \hat{U}_{2,2}A^2(\mathrm{e}^{2\mathrm{i}k\eta} + \text{c.c.}) + \hat{U}_{2,0}A^2, \\ \hat{V}_2 &= \hat{V}_{2,a}(\mathrm{i}\,\mathrm{e}^{\mathrm{i}k\eta} + \text{c.c.})\,\mathrm{e}^{\mathrm{i}\omega t} + \text{c.c.} + \hat{V}_{2,2}A^2(\mathrm{i}\,\mathrm{e}^{2\mathrm{i}k\eta} + \text{c.c.}), \\ \hat{P}_2 &= \hat{P}_{2,a}(\mathrm{e}^{\mathrm{i}k\eta} + \text{c.c.})\,\mathrm{e}^{\mathrm{i}\omega t} + \text{c.c.} + \hat{P}_{2,2}A^2(\mathrm{e}^{2\mathrm{i}k\eta} + \text{c.c.}) + \hat{P}_{2,0}A^2, \\ \hat{F}_2 &= \hat{F}_{2,a}(\mathrm{e}^{\mathrm{i}k\eta} + \text{c.c.})\,\mathrm{e}^{\mathrm{i}\omega t} + \text{c.c.} + \hat{F}_{2,2}A^2(\mathrm{e}^{2\mathrm{i}k\eta} + \text{c.c.}). \end{aligned}\right\} \tag{4.12}$$

The solution as well as the jump conditions across the flame are given in Appendix A. It suffices to note that

$$\hat{U}_{2,a} = \frac{\pm k P^{\pm}_{2,a}}{\mathrm{i}R_{\pm}\omega \mp k}\exp(\mp k\xi) + D^{\pm}\exp(-\mathrm{i}R_{\pm}\omega\xi). \tag{4.13}$$

The term with the coefficient proportional to D^- represents the fluctuation associated with the convected vorticity or gust in the oncoming fresh mixture. In reality, the vortical disturbance is random in both time and space. Here we have taken the specific component which has the same frequency as that of the acoustic mode of the duct, and the transverse wavenumber twice that of the D-L mode so that a resonant triad interaction takes place between them. D^+ measures the vorticity fluctuation behind the flame, and it can be expressed in terms of D^- and the forcing arising from the flame–sound interaction. It turns out that $D^+ \neq 0$ even if $D^- = 0$, implying that vorticity is generated by a longitudinal acoustic wave. Lieuwen (2001) showed that vorticity is generated as an oblique sound wave propagates through a flame. The two vorticity generation mechanisms, however, are different: that in the present study is nonlinear, involving a sound wave interacting with (the hydrodynamic field of) the flame, while that in Lieuwen (2001) is a purely linear mechanism.

In addition to the vortical disturbance, entropic perturbations in the oncoming flow may also interact with the flame to generate sound. However, it turns out that an entirely self-consistent treatment of this effect requires a substantial reformulation

of the theory at the onset. This has been done already and will be published in a forthcoming paper.

We now proceed to the cubic order, and the governing equations are found to be

$$\frac{\partial \hat{U}_3}{\partial \xi} + \frac{\partial \hat{V}_3}{\partial \eta} = \frac{\partial \hat{V}_1}{\partial \xi}\frac{\partial \hat{F}_2}{\partial \eta} + \frac{\partial \hat{V}_2}{\partial \xi}\frac{\partial \hat{F}_1}{\partial \eta}, \tag{4.14}$$

$$\begin{aligned} R\frac{\partial \hat{U}_3}{\partial t} + \frac{\partial \hat{U}_3}{\partial \xi} = &-\frac{\partial \hat{P}_3}{\partial \xi} - RA'\hat{U}_{1,\tau} - R\left\{\hat{U}_1\frac{\partial \hat{U}_2}{\partial \xi} + \hat{U}_2\frac{\partial \hat{U}_1}{\partial \xi} + \hat{V}_1\frac{\partial \hat{U}_2}{\partial \eta} + \hat{V}_2\frac{\partial \hat{U}_1}{\partial \eta}\right\} \\ &+ R\left\{\hat{F}_{0,\tau} + \hat{F}_2' + \hat{V}_1\frac{\partial \hat{F}_1}{\partial \eta}\right\}\frac{\partial \hat{U}_1}{\partial \xi} - R\hat{\mathscr{J}}h(\xi)\frac{\partial \hat{U}_1}{\partial \xi} + Pr\nabla^2\hat{U}_1, \end{aligned} \tag{4.15}$$

$$\begin{aligned} R\frac{\partial \hat{V}_3}{\partial t} + \frac{\partial \hat{V}_3}{\partial \xi} = &-\frac{\partial \hat{P}_3}{\partial \eta} - RA\hat{V}_{1,\tau} - R\left\{\hat{U}_1\frac{\partial \hat{V}_2}{\partial \xi} + \hat{U}_2\frac{\partial \hat{V}_1}{\partial \xi} + \hat{V}_1\frac{\partial \hat{V}_2}{\partial \eta} + \hat{V}_2\frac{\partial \hat{V}_1}{\partial \eta}\right\} \\ &+ R\left\{\hat{F}_{0,\tau} + \hat{F}_2' + \hat{V}_1\frac{\partial \hat{F}_1}{\partial \eta}\right\}\frac{\partial \hat{V}_1}{\partial \xi} - R\hat{\mathscr{J}}h(\xi)\frac{\partial \hat{V}_1}{\partial \xi} + Pr\nabla^2\hat{V}_1 \\ &+ \frac{\partial \hat{P}_1}{\partial \xi}\frac{\partial \hat{F}_2}{\partial \eta} + \frac{\partial \hat{P}_2}{\partial \xi}\frac{\partial \hat{F}_1}{\partial \eta}, \end{aligned} \tag{4.16}$$

where $\hat{\mathscr{J}} = qk^2A^2$. At this order, it is only necessary to consider the component which coincides with the fundamental of the D-L mode, and thus we write

$$\left.\begin{aligned} &(\hat{U}_3, \hat{P}_3, \hat{F}_3) = (\hat{U}_{3,1}, \hat{P}_{3,1}, \hat{F}_{3,1})(\mathrm{e}^{\mathrm{i}k\eta} + \text{c.c.}), \\ &\hat{V}_3 = \hat{V}_{3,1}(\mathrm{i}\,\mathrm{e}^{\mathrm{i}k\eta} + \text{c.c.}). \end{aligned}\right\} \tag{4.17}$$

The solution for $\hat{P}_{3,1}$, $\hat{U}_{3,1}$ and $\hat{V}_{3,1}$ are given by (A 10)–(A 12) in Appendix A.

The jump conditions and the front equation at this order need some attention. A direct expansion of (3.15), (3.18) and (3.12) shows that at $O(\epsilon^3)$,

$$\left.\begin{aligned} [\hat{U}_3] &= -q\nabla\hat{F}_1\cdot\nabla\hat{F}_2, \\ [\hat{V}_3] &= -q\nabla\hat{F}_3 + \tfrac{1}{2}q(\nabla\hat{F}_1)^2\nabla\hat{F}_1, \\ [\hat{P}_3] &= (R_+ - R_-)(G_c\hat{F}_3 + g_d\hat{F}_1 + B\tilde{u}'_{a,1}(0,t)\hat{F}_2), \end{aligned}\right\} \tag{4.18}$$

$$\hat{F}_{1,\tau} + \hat{F}_{3,t} = \hat{U}_3(0^-, \eta, t) - \hat{V}_1\cdot\nabla\hat{F}_2 - \hat{V}_2\cdot\nabla\hat{F}_1 - \nabla\hat{F}_1\cdot\nabla\hat{F}_2. \tag{4.19}$$

However, since we assume that $\delta = O(\epsilon^2)$, the $(\epsilon\delta)$ terms in (2.15) are of the same order as the $O(\epsilon^3)$ terms in the expansion (4.6). They must then be combined to give

$$\left.\begin{aligned} [\hat{U}_{3,1}] &= \tfrac{1}{2}lqD(q)k^2A - 2qk^2\hat{F}_{2,2}A^3, \\ [\hat{V}_{3,1}] &= -kq\hat{F}_{3,1} + \chi qk^2A + \tfrac{3}{2}qk^3A^3, \\ [\hat{P}_{3,1}] &= -lqD(q)k^2A - qk^2A \\ &\quad + (R_+ - R_-)[G_c\hat{F}_3 + g_dA + (\mathrm{i}\omega\hat{F}_{2,a}\hat{u}_{a,1}(0)B + \text{c.c.})], \end{aligned}\right\} \tag{4.20}$$

$$A' = \hat{U}_{3,1}(0^-) - 2k^2\hat{F}_{2,2}A^3 - k\hat{V}_{2,2}(0^-)A^3 - k^2\left\{\frac{1+q}{q}\ln(1+q) + \tfrac{1}{2}lD(q)\right\}A. \tag{4.21}$$

Inserting into (4.20) and (4.21) the solution for $\hat{P}_{3,1}$, $\hat{U}_{3,1}$, we obtain the system

$$\boldsymbol{M\alpha} = \boldsymbol{b}, \tag{4.22}$$

for $\boldsymbol{\alpha} = (P^+_{3,1}, P^-_{3,1}, \hat{F}_{3,1}, C^+_{3,1})$, where the matrix

$$\boldsymbol{M} = \begin{bmatrix} 1 & -1 & qk & 0 \\ -1 & 1 & 0 & 1 \\ 1 & 1 & qk & 0 \\ 0 & -1 & 0 & 0 \end{bmatrix}, \tag{4.23}$$

and the inhomogeneous term $\boldsymbol{b} = (b_1, b_2, b_3, b_4)^T$ is given by

$$\begin{aligned}
b_1 &= A^3\{R_+(2P^+_{2,2} + 2R_+P^2 - \tfrac{16}{3}kP)P - \tfrac{4}{3}R_+P^+_{2,2}P + 2(P^+_{2,2} + P^-_{2,2})k\} \\
&\quad - (R_+ - R_-)(\mathrm{i}\omega\hat{F}_{2,a}\hat{u}^*_{a,1}(0)B^* + \text{c.c.}) - \frac{qg_d}{1+q}A - lqD(q)k^2A - qk^2A, \\
b_3 &= A^3\{R_+(R_+P^2 - 5kP)P + R_+(C^+_{2,2} + qk^2 + k^2)P + \tfrac{1}{3}R_+P^+_{2,2}P + \tfrac{2}{3}R^2_+P^3 \\
&\quad - 2kP\hat{F}_{2,2} + 2k(P^+_{2,2} - P^-_{2,2}) + \tfrac{3}{2}qk^3\} + \ln(1+q)(kG_c)A, \\
b_4 &= A' + (kP^-_{2,2} + 2k^2\hat{F}_{2,2})A^3 + k^2\left\{\frac{1+q}{q}\ln(1+q) + \tfrac{1}{2}lD(q)\right\}A.
\end{aligned}$$

The expression for b_2 is omitted since it is not needed. Because the matrix $\boldsymbol{M}$ is singular, (4.22) has a solution only when the solvability condition $b_3 - b_1 + 2b_4 = 0$ is satisfied, which implies that

$$A' = \kappa A + \gamma_s A^3 - \gamma_b|B|^2A + l_sD^-B^* + l^*_sD^{-*}B, \tag{4.24}$$

where the linear growth rate

$$\kappa = -\frac{q}{2(1+q)}g_d - \tfrac{1}{2}k^2\left\{q + \frac{1+q}{q}((q+2)\ln(1+q) + lqD(q))\right\}, \tag{4.25}$$

while the coefficients of the nonlinear terms are given by

$$\gamma_s = \left\{-\tfrac{1}{2}q + \tfrac{3}{2} + \frac{2}{q}\right\}k^3 = (4-q)(1+q)k^3/(2q), \tag{4.26}$$

$$\gamma_b = \frac{4(R_+ - R_-)^2(1 + R_+/R_-)k\omega^2\sin^2\left(R^{1/2}_-\sigma\omega L\right)}{(R_+ + R_-)^2\omega^2 + 4k^2}, \tag{4.27}$$

$$l_s = \frac{2(R_+ - R_-)R^{-1/2}_-(\mathrm{i}R_-\omega + k)\sin\left(R^{1/2}_-\sigma\omega L\right)}{\mathrm{i}(R_+ + R_-)\omega + 2k}. \tag{4.28}$$

4.2. *Analysis of the acoustics*

The pressure and velocity of the acoustic fluctuation are expanded as

$$p_a = \epsilon B(\tau)p_{a,1} + \epsilon^3 p_{a,2} + \ldots, \quad u_a = \epsilon B(\tau)u_{a,1} + \epsilon^3 u_{a,2} + \ldots, \tag{4.29}$$

where B is the amplitude function.

To leading-order, $p_{a,1}$ and $u_{a,1}$ satisfy (3.6), and the solution consists of sound waves travelling to the left and right, namely

$$\left.\begin{aligned}
p_{a,1} &= \exp(\mathrm{i}\omega t)\{a^\pm_r\exp(-\mathrm{i}R^{1/2}_\pm\omega\tilde{\xi}) + a^\pm_l\exp(\mathrm{i}R^{1/2}_\pm\omega\tilde{\xi})\} + \text{c.c.} \\
&\equiv \hat{p}_{a,1}\exp(\mathrm{i}\omega t) + \text{c.c.} \\
u_{a,1} &= \exp(\mathrm{i}\omega t)R^{-1/2}_\pm\{a^\pm_r\exp(-\mathrm{i}R^{1/2}_\pm\omega\tilde{\xi}) - a^\pm_l\exp(\mathrm{i}R^{1/2}_\pm\omega\tilde{\xi})\} + \text{c.c.} \\
&\equiv \hat{u}_{a,1}\exp(\mathrm{i}\omega t) + \text{c.c.}
\end{aligned}\right\}, \tag{4.30}$$

where $a_r^{\pm}$ and $a_l^{\pm}$ are constants, and for convenience we take $a_l^- = \exp(\mathrm{i}R_-^{1/2}\sigma\omega L)$. The end conditions are

$$u_{a,1} = 0 \quad \text{at} \quad \tilde{\xi} = -\sigma L, \quad p_{a,1} = 0 \quad \text{at} \quad \tilde{\xi} = (1-\sigma)L \tag{4.31}$$

where L is related to the dimensional length of the duct l^* via

$$L = Ml^*/h^*,$$

and σ is a parameter characterizing the mean position of the flame front. Both $u_{a,1}$ and $p_{a,1}$ are continuous across the flame, i.e.

$$[u_{a,1}] = 0, \quad [p_{a,1}] = 0, \tag{4.32}$$

as indicated by the expansion of (3.7). Application of these conditions leads to the dispersion relation of the acoustic mode (cf. Clavin *et al.* 1990; Pelce & Rochwerger 1992)

$$\left(\frac{R_+}{R_-}\right)^{1/2} \tan\left(R_-^{1/2}\sigma\omega L\right) \tan\left(R_+^{1/2}(1-\sigma)\omega L\right) = 1, \tag{4.33}$$

which determines the characteristic frequency of the duct.

Inserting (4.29) into (3.6), then at $O(\epsilon^3)$, we have

$$R\frac{\partial^2 p_{a,2}}{\partial t^2} - \frac{\partial^2 p_{a,2}}{\partial \tilde{\xi}^2} = -2R\mathrm{i}\omega B'(\tau)p_{a,1}, \quad R\frac{\partial u_{a,2}}{\partial t} = -\frac{\partial p_{a,2}}{\partial \tilde{\xi}} - RB'(\tau)u_{a,1}, \tag{4.34}$$

whose solutions are found to be

$$\begin{aligned} p_{a,2} = \exp(\mathrm{i}\omega t)\big\{ &\left(b_r^{\pm}\exp\left(-\mathrm{i}R_{\pm}^{1/2}\omega\tilde{\xi}\right) + b_l^{\pm}\exp\left(\mathrm{i}R_{\pm}^{1/2}\omega\tilde{\xi}\right)\right) \\ &- R_{\pm}^{1/2}B'\tilde{\xi}\left(a_r^{\pm}\exp\left(-\mathrm{i}R_{\pm}^{1/2}\omega\tilde{\xi}\right) - a_l^{\pm}\exp\left(\mathrm{i}R_{\pm}^{1/2}\omega\tilde{\xi}\right)\right)\big\} + \text{c.c.}, \\ u_{a,2} = \exp(\mathrm{i}\omega t)\big\{ &R_{\pm}^{-1/2}\left(b_r^{\pm}\exp\left(-\mathrm{i}R_{\pm}^{1/2}\omega\tilde{\xi}\right) - b_l^{\pm}\exp\left(\mathrm{i}R_{\pm}^{1/2}\omega\tilde{\xi}\right)\right) \\ &- B'\tilde{\xi}\left(a_r^{\pm}\exp\left(-\mathrm{i}R_{\pm}^{1/2}\omega\tilde{\xi}\right) + a_l^{\pm}\exp\left(\mathrm{i}R_{\pm}^{1/2}\omega\tilde{\xi}\right)\right)\big\} + \text{c.c.} \end{aligned}$$

It follows from substituting F_0 into (3.23) and expanding to $O(\epsilon^3)$ that

$$[p_{a,2}] = 0, \quad [u_{a,2}] = \left(2qk^2\hat{F}_{2,a}A + \tfrac{1}{2}q(\beta M/\epsilon^2)\hat{h}_{-\infty}\right)\mathrm{e}^{\mathrm{i}\omega t} + \text{c.c.}, \tag{4.35}$$

where $\hat{h}_{-\infty} = (\gamma-1)\hat{p}_{a,1}(0)B$. The above relations together with the end conditions, $u_{a,2} = 0$ at $\tilde{\xi} = -\sigma L$ and $p_{a,2} = 0$ at $\tilde{\xi} = (1-\sigma)L$, give rise to the following 4×4 system for $b_r^{\pm}$ and $b_l^{\pm}$:

$$\begin{bmatrix} 1 & 1 & -1 & -1 \\ 1 & -1 & -\sqrt{\frac{R_-}{R_+}} & \sqrt{\frac{R_-}{R_+}} \\ 1 & -\exp\left(-2\mathrm{i}R_-^{1/2}\sigma\omega L\right) & 0 & 0 \\ 0 & 0 & 1 & \exp\left(2\mathrm{i}R_+^{1/2}(1-\sigma)\omega L\right) \end{bmatrix} \begin{bmatrix} b_r^- \\ b_l^- \\ b_r^+ \\ b_l^+ \end{bmatrix} = \boldsymbol{d} \tag{4.36}$$

where

$$\boldsymbol{d} = \begin{bmatrix} 0 \\ -R_-^{1/2}\left(2k^2q\hat{F}_{2,a}A + \frac{1}{2}q(\beta M/\epsilon^2)\hat{h}_{-\infty}\right), \\ -R_-^{1/2}\sigma L\left(a_r^- + a_l^-\exp\left(-2\mathrm{i}R_-^{1/2}\sigma\omega l\right)\right)B', \\ R_+^{1/2}(1-\sigma)L\left(a_r^+ - a_l^+\exp\left(2\mathrm{i}R_+^{1/2}(1-\sigma)\omega L\right)\right)B'. \end{bmatrix} \tag{4.37}$$

Since the matrix on the left-hand side of (4.36) is singular due to (4.33), a solvability condition is required, which leads to the amplitude equation for the acoustic mode

$$B'(\tau) = \chi_s A^2 B + m_p B + m_s D^- A, \tag{4.38}$$

where

$$\chi_s = -\frac{\mathrm{i}2qk^3 R_-^{-1/2}(R_+ - R_-)\Lambda}{L(\mathrm{i}(R_+ + R_-)\omega + 2k)}, \quad m_s = \frac{2qk^2(\mathrm{i}R_-\omega + k)\Lambda}{\mathrm{i}\omega L(\mathrm{i}(R_+ + R_-)\omega + 2k)\sin\left(R_-^{1/2}\sigma\omega L\right)}, \tag{4.39}$$

$$m_p = \frac{\beta M(\gamma - 1)q\Lambda}{2\epsilon^2 L}\cot\left(R_-^{1/2}\omega\sigma L\right), \tag{4.40}$$

with

$$\Lambda = \frac{\tan\left(R_-^{1/2}\sigma\omega L\right)}{\sigma\sec^2\left(R_-^{1/2}\sigma\omega L\right) + (1-\sigma)(R_+/R_-)\sec^2\left(R_+^{1/2}(1-\sigma)\omega L\right)\tan^2\left(R_-^{1/2}\sigma\omega L\right)}. \tag{4.41}$$

5. Study of amplitude equations

5.1. *Comments on the acoustic–flame coupling mechanisms*

The sound–flame interaction is thus described by the system of coupled amplitude equations (4.24) and (4.38), i.e.

$$\left.\begin{aligned} A' &= \kappa A + \gamma_s A^3 - \gamma_b |B|^2 A + l_s D^- B^* + l_s^* D^{-*} B, \\ B' &= \chi_s A^2 B + m_p B + m_s D^- A. \end{aligned}\right\} \tag{5.1}$$

For the case where no vortical perturbations are present in the oncoming fresh mixture ($D^- = 0$), the amplitude equations simplify to

$$A'(\tau) = \kappa A + \gamma_s A^3 - \gamma_b |B|^2 A, \tag{5.2}$$

$$B'(\tau) = \chi_s A^2 B + m_p B. \tag{5.3}$$

The first and second terms on the right-hand side of (5.3), $\chi_s A^2 B$ and $m_p B$, represent two distinct sound amplification mechanisms: the change of flame surface area and the pressure effect, respectively. For a flat flame, $A \equiv 0$, and hence $B' = m_p B$. This reduces to the case studied by Clavin *et al.* (1990).

Now if the flame amplitude A is (artificially) taken to be a constant (and the pressure effect term is dropped), then equation (5.3) reduces to the result of Pelce & Rochwerger (1992), which predicts that sound intensity B amplifies exponentially. This captures an important aspect of Searby's experiments. However, the coupling in their model is one way, since the back effect of sound on the flame is neglected, and as a result it was incapable of describing the whole evolution process observed. The present work includes this back effect as well as the self-nonlinearity of the D-L mode. This leads to a more complete description of the experiments of Searby (1992); see below.

The effects of the nonlinear interactions transpire if we inspect the signs of the coefficients. According to (4.39) and (4.27), $\Re(\chi_s) > 0$ and $\gamma_b > 0$, indicating that the flame always acts to amplify the acoustic field, while the sound inhibits the flame. Note also that γ_s is positive (negative) for $q < 4$ ($q > 4$), and hence the self-nonlinearity of the flame is destabilizing for $q < 4$ and stabilizing for $q > 4$.

When a vortical disturbance is present in the oncoming fresh mixture, the sound–flame coupling is described by the full equations (5.1). As in aeroacoustics and unsteady aerodynamics, vortical disturbances in the form of convected gust represent

'weak turbulence'. The effect of such large-scale weak turbulence has been studied previously by Williams (1970), Clavin & Williams (1979, 1982) and Searby & Clavin (1986), with the primary interest being to predict the spectra or root-mean-squares of the fluctuations in the flame thickness and speed. All these studies were, however, restricted to stable flames, excluding any form of instability and acoustic modes. The present study appears to be the first analysis of the interaction between an external perturbation and a (marginally) unstable flame. Though the coupling terms $(l_s B^* + l_s^* B)$ and $m_s A$ in (5.1) arise because of a resonant-triad interaction between the acoustic and D-L modes mediated by the gust, i.e. the sound interacts with the gust to influence the D-L mode, and at the same time the D-L mode interacts with the gust to affect the sound.

In the analysis above, we assumed that $D^- = O(1)$, which corresponds to a vortical disturbance with small magnitude of $O(\epsilon^2)$. If $D^- \gg 1$, the triadic effect would be dominant. In fact, the triadic interaction is a distinct coupling mechanism, which in principle may operate independently. To illustrate this point, we introduce the substitutions $\tau \to \tilde{\tau}/D^-$ into (5.1) and take the limit $D^- \to \infty$. Then the amplitude equations to leading order reduce to

$$A'(\tilde{\tau}) = \tilde{\kappa} A + l_s B^* + l_s^* B, \qquad B'(\tilde{\tau}) = m_s A, \tag{5.4a, b}$$

where $\tilde{\kappa} = -(G - G_c)q/(2(1+q)\epsilon^2 D^-) = O(1)$. Elimination of B in (5.4) leads to

$$A'' = \tilde{\kappa} A' + (l_s m_s^* + l_s^* m_s) A,$$

where we have used the fact that A is real-valued. The coefficient of the second term on the right-hand side turns out to be identically zero in view of (4.39) and (4.28). Therefore, $A \sim \mathrm{e}^{\tilde{\kappa}\tilde{\tau}}$, implying that the growth of the D-L mode is actually unaffected by the coupling. It follows from (5.4*b*) that $B \sim \tilde{\kappa}^{-1} \mathrm{e}^{\tilde{\kappa}\tilde{\tau}}$, that is, the acoustic mode is 'locked' with the D-L mode through the triadic interaction. The system (5.1) then unifies the newly identified and existing mechanisms.

The present sound-generation mechanism by vortical disturbances differs from those known previously. Since it involves a nonlinear triadic interaction with the D-L mode, it clearly differs from that due to the direct interaction between acoustic and vortical modes considered in Chu & Kovasznay (1958). It is known that a convected gust with its wavefront almost perpendicular to the flame produces sound, as was pointed out by Markstein (1964). In essence, what Markstein showed was that when compressibility is included, certain D-L modes become radiating, i.e. merge with acoustic modes. They can be excited by vortical disturbances through the rather familiar linear coupling at a discontinuity (here a frame front); the surface area change due to the flame wrinkling does not play any role. The acoustic modes are neither decaying nor growing, and propagate away from both sides of the flame. Therefore the vortical disturbances lead to sound radiation rather than an acoustic instability. This is in contrast to the present mechanism, which is nonlinear as emphasized above and in which sound amplifies because of the flame surface area being modulated by the vortical disturbances.

5.2. *Numerical study of amplitude equations*

We evaluate the coefficients for the following parameter values

$$\left.\begin{array}{l} h^* = 10\,\mathrm{cm}, \quad l^* = 120\,\mathrm{cm}, \quad (R_- - R_+)/R_- = 0.84 \text{ (or equivalently } q = 5.25), \\ D_{th}^* = 0.22\,\mathrm{cm^2\,s^{-1}}, \quad a^* = 340\,\mathrm{m\,s^{-1}}, \quad Le = 0.93, \quad \beta = 12, \quad \gamma = 1.4. \end{array}\right\} \tag{5.5}$$

These parameters are chosen to be close to those in Searby's (1992) experiments, which were conducted in a 120 cm long tube with a diameter of 10 cm using premixed propane. The equivalence ratio is about $0.7 \sim 0.77$, for which the Lewis number $Le = 0.93$. The observations that are relevant for our theory correspond to laminar flame speeds $U_L = 16 \sim 25\,\mathrm{cm\,s^{-1}}$, and a typical measurement was presented in figure 3 of Searby (1992) for $U_L = 22.3\,\mathrm{cm\,s^{-1}}$. Note that for a tube, these speeds are in the supercritical regime since the critical speed is about $14.3\,\mathrm{cm\,s^{-1}}$ for the parameters given in (5.5).

In our calculation, we take the laminar flame speed $U_L = 24\,\mathrm{cm\,s^{-1}}$. This is about 9% above the critical laminar flame speed for neutral stability, which for a duct is $22.3\,\mathrm{cm\,s^{-1}}$ according to (4.1). It seems reasonable to expect the weakly nonlinear theory to be valid in such a moderate supercritical condition. The small parameter

$$\epsilon = (d/h^*)^{1/2} = (h^* U_L / D^*_{th})^{-1/2} = 0.0303.$$

Figure 2 shows the variation of the coefficients with $\hat{\sigma} \equiv (1 - \sigma)$, a parameter characterizing the mean flame position. Of particular interest is figure 2(*b*), which shows that sound amplification due to the pressure effect (as measured by m_p) is negligible in the upper half of the duct, but becomes appreciable in the lower half. The coefficient χ_s, which measures flame–sound coupling due to the change of flame surface area, peaks at a location in the lower half of the duct. This, however, does not necessarily mean that sound would be mainly generated in this region because the true contribution to sound depends also on A^2.

In general, the flame moves along the duct. Its mean position is given by

$$x_m = x_r + (U_- - 1)t - k^2 \int_0^\tau \hat{F}_0 \,\mathrm{d}\tau = x_r + (U_- - 1)t - k^2 \int_0^\tau A^2 \,\mathrm{d}\tau,$$

where x_r is a reference position of the flame at the time $\tau = 0$, and the integral term is associated with the increased flame speed due to flame curvature.

For the flame to be stationary relative to the duct, the feeding speed of the fresh mixture, U_-, must be continuously adjusted. For simplicity, we first assume this to be the case. Equation (5.1) can be integrated subject to the initial conditions

$$A = A_0, \quad B = B_0 \quad \text{at} \quad \tau = 0.$$

In the following, we take $A_0 = 1.6$ (or $\epsilon A_0 = 0.05$). In order to relate more closely with the physical quantities, the results will be presented for ϵA and ϵB in terms of the original time variable t.

The evolution of the sound and flame is shown in figure 3 for three representative flame locations corresponding to $\hat{\sigma} = 0.7$, 0.5 and 0.3. For comparison purposes, we also include the solution with the pressure effect turned off (i.e. $m_p = 0$). The D-L mode develops from an initial small disturbance and quickly saturates at constant level owing to its self-nonlinearity, leading to the formation of a cured flame. The increased flame surface then causes sound to amplify rapidly. As sound reaches a certain intensity, it stabilizes the D-L mode via the feedback term $\gamma_b |B^2| A$ in (5.3), causing the flame to flatten. The sound then amplifies at a much smaller rate owing to the pressure effect, or saturates if that effect is ignored. Note that here we have neglected any acoustic loss. In reality, the sound level in the later stage should be between the predictions with and without the pressure. Overall, the theoretical results are reminiscent of the observations of Searby (1992); a more detailed comparison will

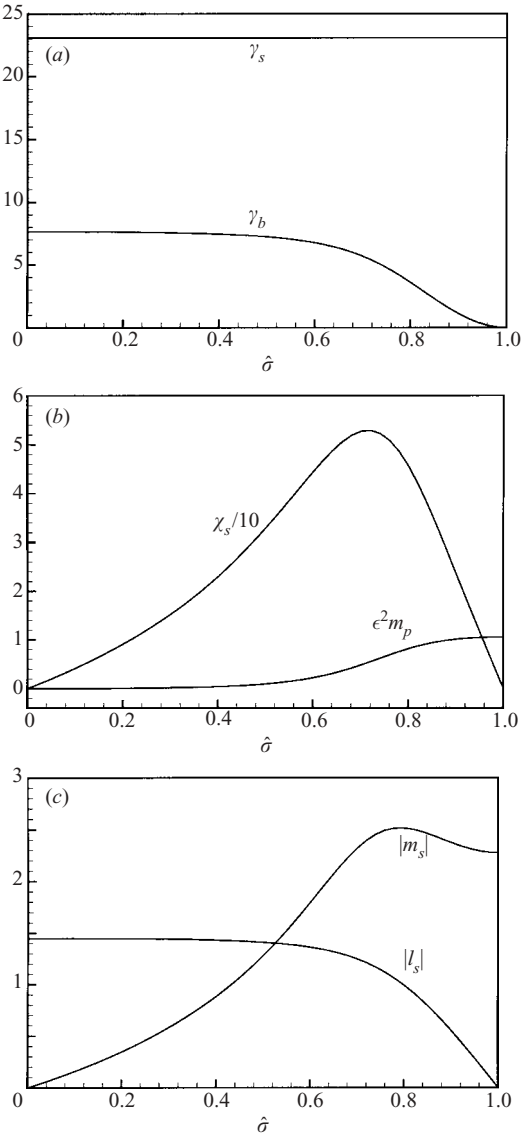

FIGURE 2. Variation of coefficients with $\hat{\sigma}$: (*a*) γ_s and γ_b, (*b*) χ_s and m_p, and (*c*) l_s and m_s.

be given later. The predicted stabilization of D-L instability by the relatively weak pressure fluctuation is also consistent with the experiment of Searby & Rochwerger (1991).

The coupling through the pressure effect on the burning rate is of secondary importance, consistent with the conclusion of Pelce & Rochwerger (1992). For flames anchored in the upper half of the duct, the pressure effect is minor and manifests itself only after the flame reverts to a flat state. Relatively speaking, this effect is more pronounced for flames anchored in the lower half of the duct.

To examine the effect of the background sound level on the solution, in figure 4, we compare the results for three different values of B_0. As B_0 increases, sound reaches

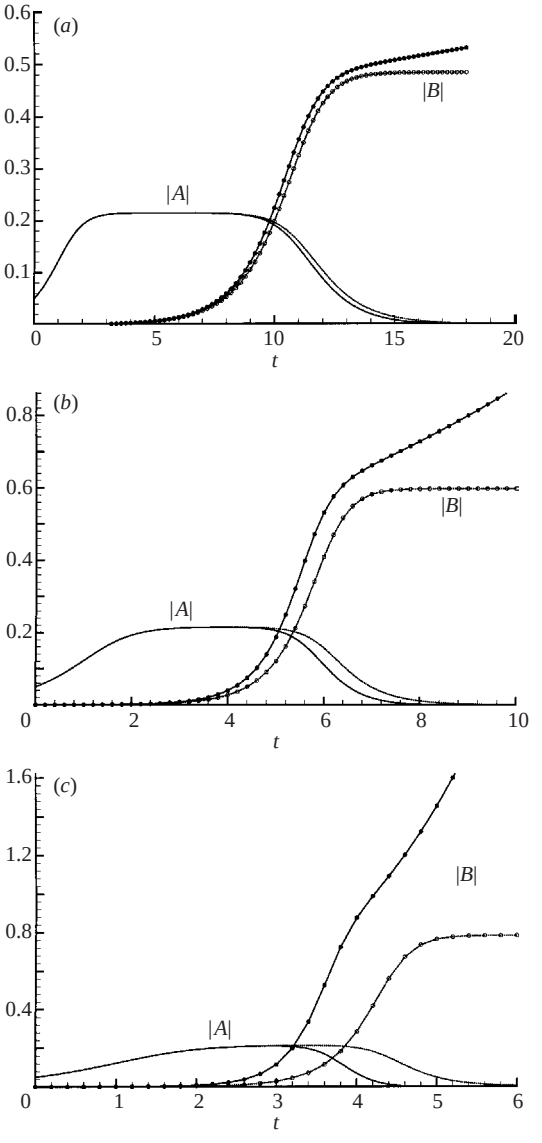

FIGURE 3. Nonlinear evolution of the acoustic amplitude ϵB and flame amplitude ϵA: (*a*) $\widehat{\sigma} = 0.3$, (*b*) $\widehat{\sigma} = 0.5$ and (*c*) $\widehat{\sigma} = 0.7$. The parameter $\epsilon B_0 = 0.5 \times 10^{-3}$. The dotted lines represent the results for $m_p = 0$.

a large amplitude earlier, as expected, and as a consequence flame flattening also occurs sooner. The overall behaviour is not altered by B_0. Though not shown here, increasing A_0 has a similar effect.

Figure 5 shows the evolution of the flame and sound when vortical disturbances are present in the oncoming flow. As illustrated, these disturbances prompt sound amplification at an earlier stage. If sufficiently strong ($\epsilon^2 D^- \geqslant 0.01$), they may prevent the flame from saturating. The apparent resemblance between figures 4 and 5 indicates that the effect of increasing the magnitude of the vortical disturbances is similar to that of increasing the background sound level.

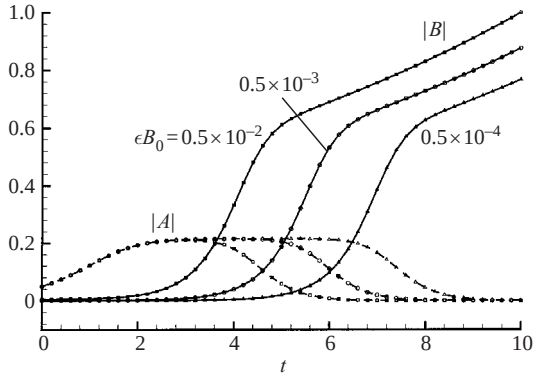

FIGURE 4. Nonlinear evolution of the acoustic amplitude ϵB and flame amplitude ϵA for $\epsilon B_0 = 0.5 \times 10^{-2}$, 0.5×10^{-3} and 0.5×10^{-4}. The flame position corresponds to $\widehat{\sigma} = 0.5$.

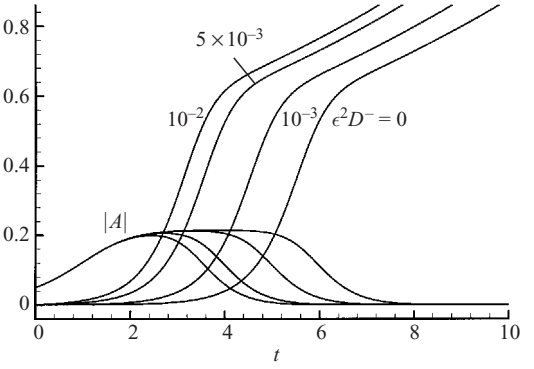

FIGURE 5. Nonlinear evolution of the acoustic amplitude ϵB and flame amplitude ϵA when the vortical disturbance amplitude $\epsilon^2 D^- = 0$, 0.001, 0.005 and 0.01. The parameter $\epsilon B_0 = 0.5 \times 10^{-3}$.

We now turn to the situation where the flame moves along the duct, with particular reference to Searby's (1992) experiments, where the flame propagates into the fresh mixture at rest and so $U_- = 0$. If we assume that the flame is at the exit end of the duct at $\tau = 0$, then $x_r = L/M$, and the parameter $\widehat{\sigma} = (1 - \sigma)$ is related to the time by the relation

$$\widehat{\sigma} = 1 - \sigma = \frac{M}{\epsilon^2 L}\left(\tau + \epsilon^2 k^2 \int_0^\tau |A|^2 \, \mathrm{d}\tau\right). \tag{5.6}$$

As a result, the frequency of the acoustic mode changes with the position and hence with time, and so do the coefficients in (5.1)–(5.3). This time dependence is parametric provided that $\epsilon^2 \gg M$, that is, at each location, these coefficients, as well as the frequency of the acoustic mode, can be calculated by treating σ as a parameter.

We may include the effect of the slow variation by coupling the frequency and coefficients with the amplitudes. The can be done by using $\widehat{\sigma} \equiv (1 - \sigma)$, which is a measure of the distance of the flame to the exit end, as an independent variable. Performing the variable substitution $\widehat{\sigma} = M\tau/(\epsilon^2 L)$ (which is a leading-order

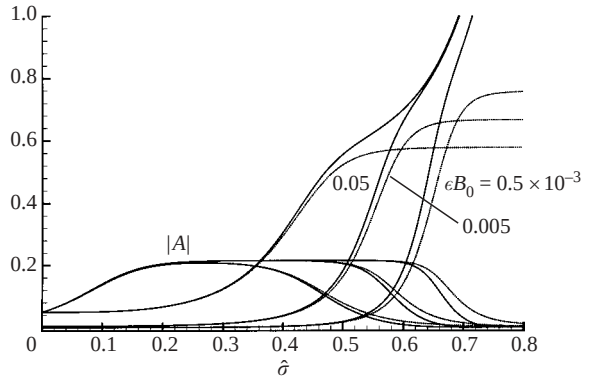

FIGURE 6. Spatial evolution of the acoustic amplitude ϵB and flame amplitude ϵA. The parameter $\epsilon B_0 = 0.5 \times 10^{-1}$, 0.5×10^{-2} and 0.5×10^{-3}. The dotted lines represent the results with $m_p = 0$.

approximation of (5.6)) in (5.1), we obtain

$$\left.\begin{aligned} \frac{\mathrm{d}A}{\mathrm{d}\hat{\sigma}} &= \frac{\epsilon^2 L}{M}(\kappa A + \gamma_s A^3 - \gamma_b |B|^2 A + l_s D^- B^* + l_s^* D^{-*} B), \\ \frac{\mathrm{d}B}{\mathrm{d}\hat{\sigma}} &= \frac{\epsilon^2 L}{M}(\chi_s A^2 B + m_p B + m_s D^- A), \end{aligned}\right\} \tag{5.7}$$

where $0 \leqslant \hat{\sigma} \leqslant 1$, and the coefficients γ_b, χ_s, l_s, m_s and m_p are functions of $\hat{\sigma}$. The initial conditions, $A = A_0$ and $B = B_0$, are imposed at $\hat{\sigma} = 0$.

Once A is solved from (5.7) as a function of $\hat{\sigma}$, we may then find the corresponding time from

$$t = \tau/\epsilon^2 = \frac{L}{M}\int_0^{\hat{\sigma}} \frac{\mathrm{d}\hat{\sigma}}{1 + \epsilon^2 k^2 A^2(\hat{\sigma})}. \tag{5.8}$$

In figure 6, we show how sound and flame evolve along the duct for three different values of B_0. The main feature is the same as for anchored flames shown in figure 3. For sufficiently small B_0, sound attains significant intensity only after it reaches the lower half of the duct. However, for increased values of B_0, major sound amplification may occur in the upper half of the duct. Therefore, the peak position of the coupling coefficient χ_s (see figure 2*b*) does not dictate where intense sound is produced.

The theoretical results in figure 6 capture qualitatively the behaviours of flame and sound as observed by Searby (1992). This is achieved by including the two-way coupling between the flame and sound. To relate our theoretical prediction more directly to Searby's measurement, we calculate the amplitude of acoustic pressure at the duct end. In the dimensional form, this pressure is

$$p_e \equiv \left(\rho_{-\infty} U_L^2\right) M^{-1} \max |p_a(-\sigma L)| = 4\epsilon |B| \left(\rho_{-\infty} U_L^2\right)/M,$$

where we take the density of the premixed propane $\rho_{-\infty} = 1.789\,\mathrm{kg\,m^{-3}}$. Using the relation (5.8), we can plot p_e and the flame position against the dimensional time. The results are shown in figure 7, while Searby's measurement is reproduced in figure 8. In experiments, the flame travels through the tube in about 3.5 s, compared with 4.2 s in our calculation. As the flame moves, the local characteristic frequency of the duct slowly changes, and at the end of the abrupt jump ($\hat{\sigma} = 0.58$) the frequency is about 130 Hz, which was the frequency recorded by Searby (1992). When the pressure

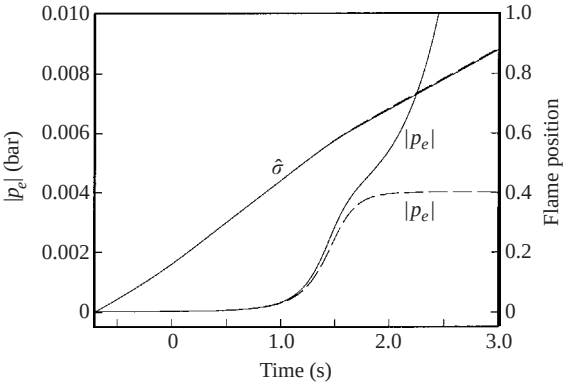

FIGURE 7. Time variation of the flame position and the acoustic pressure at the end of the duct. The parameters $D^- = 0$ and $\epsilon B_0 = 0.5 \times 10^{-2}$. The dashed lines show the results with $m_p = 0$.

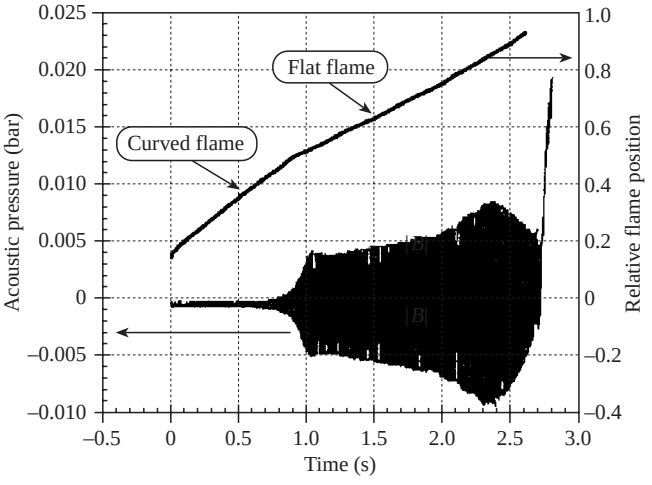

FIGURE 8. Time traces of the acoustic pressure and the flame position from Searby's experiment (figure 3*b* of Searby 1992).

effect is neglected, the theory predicts that sound saturates at about 0.004 bar, while in experiments, sound exhibits a quasi-saturation approximately at this level. With the pressure effect included, the theory significantly over predicts. As we commented above, this is because our theory ignores the acoustic loss that inevitably presents. The measured value seems to be closer to the theoretical result without the pressure effect, suggesting that the pressure effect may just offset the acoustic lose. With due allowance given to this fact, it may be said that the two sets of data are fairly close even in quantitative sense. For an entirely appropriate quantitative comparison, it is necessary to perform an analogous analysis for a tube.

Finally, figure 9 shows representative results when vortical fluctuations are present. As for anchored flames, convected vorticity tends to cause sound amplification to occur earlier; but moving flames appear to be less sensitive to these perturbations. For instance, we find that the result for $\epsilon^2 D^- = 0.001$ is indistinguishable from that for $D^- = 0$.

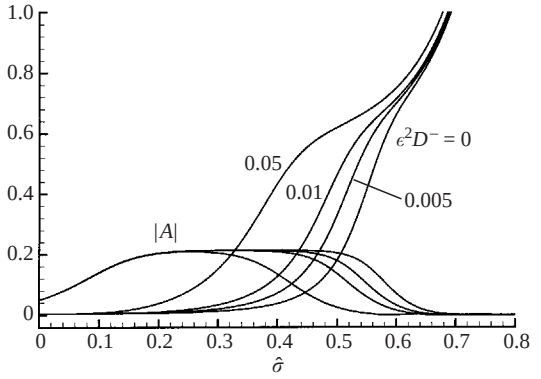

FIGURE 9. Spatial evolution of the acoustic amplitude ϵB and flame amplitude ϵA, when the vortical disturbance amplitude $\epsilon^2 D^- = 0$, 0.005, 0.01 and 0.05. The parameter $B_0 = 0.5 \times 10^{-2}$.

6. Discussion and conclusions

In this paper, the acoustic–flame coupling, the key process underlying large-scale combustion instability, is studied by using the matched asymptotic expansion techniques based on the assumptions of large activation energy and low Mach number. A general asymptotic formulation was given for the lower-frequency regime of practical relevance. In addition to its computational advantage, this formulation itself sheds useful light on the nature of flame–acoustic interaction. It shows that flame wrinkling over the acoustic time scale of the duct would definitely produce sound. On the other hand, the acoustic field so produced acts on the hydrodynamic field of the flame.

The basic framework was then used to study the weakly nonlinear interaction between an acoustic mode of the duct and a nearly neutral D-L instability mode. A system of coupled amplitude equations was derived, and was found to be able to describe the experimental observations of Searby (1992) qualitatively.

Our analysis also included the effect of vortical disturbances, which represent weak turbulence, in the oncoming fresh mixture. It is found that certain vortical perturbation may form a resonant triad with the acoustic and D-L modes. Such a triadic resonant interaction stands as a new mechanism for the sound–flame coupling.

Furthermore, the present study extended the analysis of the coupling via the direct pressure effect for a flat flame to that for a curved flame. The final coupled amplitude equations unify all three acoustic–flame coupling mechanisms.

It would be interesting to solve the fully nonlinear system (i.e. (3.9)–(3.12) coupled with (3.6) via (3.7) and (3.15)) numerically with a view to address whether or not the coupling leads to self-sustained large-amplitude pressure oscillations. The present study focused on what Searby (1992) called 'primary instability', where sound eventually suppressed the wrinkled flame. For flames of relatively high equivalence ratios, Searby (1992) observed that a second regime of instability emerged, where acoustic pressure triggers parametric instability of the flame, which in turn produces intense sound. The parametric instability induced by an externally imposed pressure field was studied by Searby & Rochwerger (1991), but the two-way coupling between the parametric instability and sound, which clearly takes place in the second regime in Searby's (1992) experiments, has not been investigated. We believe that numerical solutions of the fully nonlinear system would provide a satisfactory answer to this question.

Our theory has been formulated specifically for the situation where the sound is self-generated, but the problem of flames subject to finite-amplitude external acoustic perturbation is a closely related and interesting topic. A pressure oscillation of moderate level leads to parametric instability (Searby & Rochwerger 1991), but interestingly at sufficiently high amplitude, it restabilizes D-L instability and may even control the mean shape of a flame: a conic flame may transform into a hemispherical flame as the pressure is increased (Durox *et al.* 1997). Further experimental studies of Bourehla & Baillot (1998) reveal that the flame exhibits a rich variety of behaviours depending on the amplitude and frequency of the acoustic pressure, and they mapped out the distinct regimes in the frequency-amplitude plane. It certainly would be interesting to develop an appropriate asymptotic theory to explain these observations from first principles.

We would like to thank Dr Heinz Pitsch and Cliff Wall for helpful discussions. The work of X. W. was carried out while he was visiting the Center of Turbulence Research, Stanford University, in 2001 as a Senior Research Fellow. The referees are thanked for their detailed comments and suggestions, which have led to the improvement of the present work.

Appendix A. Details of calculations

A.1. *The solution at* $O(\epsilon^2)$

The solution for $\hat{P}_{2,a}$, $\hat{U}_{2,a}$ and $\hat{V}_{2,a}$ in (4.12) can be written as

$$\left.\begin{aligned}
\hat{P}_{2,a} &= P_{2,a}^{\pm}\exp(\mp k\xi),\\
\hat{U}_{2,a} &= \frac{\pm k P_{2,a}^{\pm}}{\mathrm{i}R_{\pm}\omega \mp k}\exp(\mp k\xi) + D^{\pm}\exp(-\mathrm{i}R_{\pm}\omega\xi),\\
\hat{V}_{2,a} &= \frac{-k P_{2,a}^{\pm}}{\mathrm{i}R_{\pm}\omega \mp k}\exp(\mp k\xi) - \frac{\mathrm{i}R_{\pm}\omega}{k}D^{\pm}\exp(-\mathrm{i}R_{\pm}\omega\xi),
\end{aligned}\right\} \tag{A 1}$$

where the terms with coefficient proportional to D^- represent the vortical fluctuations in the oncoming fresh mixture. It follows the jump conditions (4.11) and (4.10) that

$$\left.\begin{aligned}
&P_{2,a}^{+} - P_{2,a}^{-} = (R_+ - R_-)(G_c\hat{F}_{2,a} + \mathrm{i}\omega\hat{u}_{a,1}(0)AB),\\
&\frac{kP_{2,a}^{+}}{\mathrm{i}\omega R_+ - k} + D^{+} = -\frac{kP_{2,a}^{-}}{\mathrm{i}\omega R_- + k} + D^{-},\\
&-\frac{kP_{2,a}^{+}}{\mathrm{i}\omega R_+ - k} - \frac{\mathrm{i}\omega R_+}{k}D^{+} = -\frac{kP_{2,a}^{-}}{\mathrm{i}\omega R_- + k} - \frac{\mathrm{i}\omega R_-}{k}D^{-} - qk\hat{F}_{2,a},\\
&\mathrm{i}\omega\hat{F}_{2,a} = -\frac{kP_{2,a}^{-}}{\mathrm{i}\omega R_- + k} + D^{-}.
\end{aligned}\right\} \tag{A 2}$$

Solving these equations, we find

$$\hat{F}_{2,a} = (\mathrm{i}\omega)^{-1}\frac{2(\mathrm{i}\omega R_- + k)}{\mathrm{i}\omega(R_- + R_+) + 2k}D^{-} + \frac{k\hat{u}_{a,1}(0)(R_+ - R_-)AB}{\mathrm{i}\omega(R_- + R_+) + 2k}. \tag{A 3}$$

The solution for the harmonic component is given by

$$\left.\begin{aligned}
\hat{P}_{2,2} &= P_{2,2}^{\pm}\,\mathrm{e}^{\mp 2k\xi} + \left\{\tfrac{2}{3}P^2R_+ - kP\right\}h(\xi)\,\mathrm{e}^{-k\xi} - R_{\pm}G_c\hat{F}_{2,2},\\
\hat{U}_{2,2} &= -P_{2,2}^{\pm}\,\mathrm{e}^{\mp 2k\xi} - \left\{\tfrac{2}{3}P^2R_+ - kP\right\}h(\xi)\,\mathrm{e}^{-k\xi} + C_{2,2}^{\pm},\\
\hat{V}_{2,2} &= \pm P_{2,2}^{\pm}\,\mathrm{e}^{\mp 2k\xi} + \left\{\tfrac{1}{3}P^2R_+ - kP\right\}h(\xi)\,\mathrm{e}^{-k\xi}.
\end{aligned}\right\} \tag{A 4}$$

It follows from the front equation that

$$P^{-}_{2,2} = \tfrac{1}{2}k^2, \tag{A 5}$$

while the jump conditions give rise to the following relations

$$\left.\begin{aligned} &P^{+}_{2,2} + \tfrac{2}{3}R_+P^2 - kP = P^{-}_{2,2} + (R_+ - R_-)G_c\hat{F}_{2,2},\\ &-P^{+}_{2,2} - \tfrac{2}{3}R_+P^2 + kP + C^{+}_{2,2} = -P^{-}_{2,2} + \tfrac{1}{2}qk^2,\\ &P^{+}_{2,2} + \tfrac{1}{3}R_+P^2 - kP = -P^{-}_{2,2} - 2qk\hat{F}_{2,2}, \end{aligned}\right\} \tag{A 6}$$

from which we obtain

$$\left.\begin{aligned} \hat{F}_{2,2} &= \left(\frac{1}{3}\frac{q}{1+q} - \frac{1}{q}\right)k,\\ C^{+}_{2,2} &= -\left(\frac{1}{3}\frac{q^2}{1+q} - 1\right)k^2 + \tfrac{1}{2}qk^2,\\ P^{+}_{2,2} &= \left\{-\frac{q^2}{1+q} - q + \tfrac{3}{2}\right\}k^2. \end{aligned}\right\} \tag{A 7}$$

The solution for the mean-flow distortion is:

$$\left.\begin{aligned} &\hat{P}_{2,0} = P^{\pm}_{2,0} + \{-2R_+P^2\,\mathrm{e}^{-2k\xi} + (4R_+P^2 - 2kP)\,\mathrm{e}^{-k\xi}\}h(\xi),\\ &\hat{U}_{2,0} = 2kP\,\mathrm{e}^{-k\xi}\,h(\xi) + C^{\pm}_{2,0}, \end{aligned}\right\} \tag{A 8}$$

where $P^{+}_{2,0} = 0$, $C^{-}_{2,0} = 0$ in order to satisfy, respectively, the constant pressure condition at the exit, and the zero velocity condition upstream. The jump conditions for the mean-flow distortion gives the relations

$$C^{+}_{2,0} = -2kP - 2qk^2 = 0, \quad P^{-}_{2,0} = 2R_+P^2 - 2kP, \quad \hat{F}_{0,\tau} = -k^2A^2. \tag{A 9}$$

The result shows that unsteady heat release produces a mean pressure ahead of the flame front.

A.2. *The solution at* $O(\epsilon^3)$

On substituting the leading- and second-order solutions, (4.6) and (4.12), into the right-hand sides of (4.14)–(4.16), the solution for $\hat{P}_{3,1}$, $\hat{U}_{3,1}$ and $\hat{V}_{3,1}$ can readily be written as follow:

$$\begin{aligned} \hat{P}_{3,1} = {} & P^{\pm}_{3,1}\,\mathrm{e}^{\mp k\xi} \mp 2kP^{\pm}_{2,2}A^3\,\mathrm{e}^{\mp 2k\xi} + A^3\{-R_+(2P^{+}_{2,2}\,\mathrm{e}^{-k\xi} + 2R_+P^2 - \tfrac{16}{3}kP)P\,\mathrm{e}^{-2k\xi}\\ & + R_+(-2C^{+}_{2,2} + \tfrac{1}{3}R_+P^2 + 2kP)kP\xi\,\mathrm{e}^{-k\xi}\\ & - kPk^2\xi\,\mathrm{e}^{-k\xi} + \tfrac{4}{3}R_+PP^{+}_{2,2}\,\mathrm{e}^{-2k\xi}\}h(\xi), \end{aligned} \tag{A 10}$$

$$\begin{aligned} \hat{U}_{3,1} = {} & -\hat{P}_{3,1} + A^3R_+\{(-2P^{+}_{2,2}\,\mathrm{e}^{-k\xi} - \tfrac{3}{2}R_+P^2 + 4kP)P\,\mathrm{e}^{-2k\xi} + (3C^{+}_{2,2} + qk^2 + k^2)P\,\mathrm{e}^{-k\xi}\\ & + (\tfrac{3}{2}P^{+}_{2,2}\,\mathrm{e}^{-2k\xi} + R_+P^2\,\mathrm{e}^{-k\xi} - 4kP\,\mathrm{e}^{-k\xi})P\}h(\xi)\\ & + \{-A'R_+P(\xi + k^{-1}\,\mathrm{e}^{-k\xi}) - PrkP^2\xi A\}h(\xi) + C^{\pm}_{3,1}, \end{aligned} \tag{A 11}$$

$$\begin{aligned} \hat{V}_{3,1} = {} & \pm P^{\pm}_{3,1}\,\mathrm{e}^{\mp k\xi} - 2kP^{\pm}_{2,2}A^3\,\mathrm{e}^{\mp 2k\xi} - A^3R_+\{(R_+P^2 - \tfrac{8}{3}kP)P\,\mathrm{e}^{-2k\xi} - \tfrac{1}{3}PP^{+}_{2,2}\,\mathrm{e}^{-2k\xi}\\ & + (\tfrac{7}{3}kP^2 - \tfrac{2}{3}R_+P^3)\,\mathrm{e}^{-k\xi} - (C^{+}_{2,2} + qk^2 + k^2)P\,\mathrm{e}^{-k\xi} + 2kP\hat{F}_{2,2}/R_+\}h(\xi)\\ & + \{-k^{-1}A'R_+P(1 - \mathrm{e}^{-k\xi}) - PrkPA\}h(\xi). \end{aligned} \tag{A 12}$$

Here, $C^{-}_{3,1} = 0$ so that $\hat{U}_{3,1}$ satisfies the upstream condition. Note that $\hat{U}_{3,1}$ contains a term proportional to ξ and is therefore unbounded as $\xi \to \infty$. In Appendix B, we show that it eventually decays to zero in a thicker layer.

Appendix B. Buffer layer

As is implied by (4.6), the longitudinal velocity of a nearly neutral D-L mode does not decay to zero as $\xi \to \infty$. We now show that it does in a thicker 'buffer layer' with an $O(\epsilon^{-2}h^*)$ width, where the slow-time variation balances advection (and the viscous) effect(s). The relevant variable is $\xi^\dagger = \epsilon^2\xi$, and the solution expands as

$$U_0 = \epsilon\, U_1^\dagger(\mathrm{e}^{\mathrm{i}k\eta} + \text{c.c.}) + \ldots, \quad V_0 = \epsilon^3 V_1^\dagger + \ldots, \quad P_0 = \epsilon^2 P_2^\dagger(\tau) + \ldots.$$

Substitution into (3.9)–(3.11) yields the governing equations

$$R\frac{\partial U_1^\dagger}{\partial \tau} + \frac{\partial U_1^\dagger}{\partial \xi^\dagger} = -Prk^2 U_1^\dagger,$$

$$R\frac{\partial V_1^\dagger}{\partial \tau} + \frac{\partial V_1^\dagger}{\partial \xi^\dagger} = -Prk^2 V_1^\dagger, \quad \frac{\partial U_1^\dagger}{\partial \xi^\dagger} - kV_1^\dagger = 0.$$

The solution for $U_1^\dagger$ which satisfies the required matching condition

$$U_1^\dagger \to -qkA(\tau) \quad \text{as} \quad \xi^\dagger \to 0,$$

is found to be

$$U_1^\dagger = -qkA(\tau - R_+\xi^\dagger)\exp(-k^2Pr\xi^\dagger).$$

Though $V_1^\dagger$ seems over specified, it has the solution

$$V_1^\dagger = qR_+A'(\tau - R_+\xi^\dagger)\exp(-k^2Pr\xi^\dagger)$$

which is consistent with both equations. It follows that as $\xi^\dagger \to 0$,

$$V_1^\dagger \to qR_+A', \qquad U_1^\dagger \to (-qkA) + \epsilon^2(qkR_+A' + Prk^3A)\xi.$$

Thus, $V_1^\dagger$ matches $\hat{V}_{31}$, while the term proportional to ξ in $U_1^\dagger$ matches the analogous term in $\hat{U}_{31}$.

REFERENCES

Bloxsidge, G. J., Dowling, A. P. & Langhorne, P. J. 1988 Reheat buzz: an acoustically coupled combustion instability. Part 2. Theory. *J. Fluid Mech.* **193**, 445–473.

Bourehla, A. & Baillot, F. 1998 Appearance and stability of a laminar conical premixed flame subjected to an acoustic perturbation. *Combust. Flame* **114**, 303–318.

Chu, B.-T. & Kovasznay, L. S. 1958 Nonlinear interactions in a viscous heat-conducting compressible gas. *J. Fluid Mech.* **3**, 494–514.

Clavin, P. 1985 Dynamics behaviour of premixed flame fronts in laminar and turbulent flows. *Prog. Energy Combust. Sci.* **11**, 1–59.

Clavin, P. 1994 Premixed combustion and gasdynamics. *Annu. Rev. Fluid Mech.* **26**, 321–352.

Clavin, P., Pelce, P. & He, L. 1990 One-Dimensional vibratory instability of planar flames propagating in tubes. *J. Fluid Mech.* **216**, 299–322.

Clavin, P. & Williams, F. A. 1979 Theory of premixed flame propagation in large-scale turbulence. *J. Fluid Mech.* **90**, 589–604.

Clavin, P. & Williams, F. A. 1982 Effects of molecular diffusion and of thermal expansion on the structure and dynamics of premixed flames in turbulent flows of large scale and low intensity. *J. Fluid Mech.* **116**, 251–282.

Dowling, A. P. 1995 The calculation of thermoacoustic oscillations. *J. Sound Vib.* **180**, 557–581.

Dowling, A. P. 1997 Nonlinear self-excited oscillations of a ducted flame. *J. Fluid Mech.* **346**, 271–290.

Dowling, A. P. 1999 A kinematic model of a ducted flame. *J. Fluid Mech.* **394**, 51–72.

Ducruix, S., Durox, D. & Candel, S. 2000 Theoretical and experimental determination of the transfer function of laminar premixed flame. *Proc. Combust. Inst.* **28**, 765–773.

Durox, D., Baillot, F., Searby, G. & Boyer, L. 1997 On the shape of flames under strong acoustic forcing: a mean flow controlled by an oscillatory flow. *J. Fluid Mech.* **350**, 295–310.

Fleifil, M., Annaswamy, A. M., Ghoneim, Z. A. & Ghoniem, A. F. 1996 Response of a laminar premixed flame to flow oscillations: a kinematic model and thermoacoustic instability results. *Combust. Flame* **106**, 487–510.

Harten, A. V., Kapila, A. K. & Matkowsky, B. J. 1984 Acoustic coupling of flames. *SIAM J. Appl. Maths.* **44**, 982–995.

Keller, D. & Peters, N. 1994 Transient pressure effects in the evolution equation for premixed flame fronts. *Theoret. Comput. Fluid Dyn.* **6**, 141–159.

Langhorne, P. J. 1988 Reheat buzz: an acoustically coupled combustion instability. Part 1. Experiment. *J. Fluid Mech.* **193**, 417–443.

Lieuwen, T. 2001 Theoretical investigation of unsteady flow interactions with a premixed planar flame. *J. Fluid Mech.* **435**, 289–303.

Lieuwen, T. & Zinn, B. T. 1998 The role of equivalence ratio oscillations in driving combustion instabilities in low NO_x gas turbines. *Proc. Combust. Inst.* **27**, 1809–1816.

McIntosh, A. C. 1991 Pressure disturbances of different length scales interacting with conventional flames. *Combust. Sci. Technol.* **75**, 287–309.

McIntosh, A. C. 1993 The linearised response of the mass burning rate of a premixed flame to rapid pressure changes. *Combust. Sci. Technol.* **91**, 3329–3346.

McIntosh, A. C. & Wilce, S. A. 1991 High frequency pressure wave interaction with premixed flames. *Combust. Sci. Technol.* **79**, 141–155.

Markstein, G. H. 1964 *Nonsteady Flame Propagation.* Pergamon.

Markstein, G. H. 1970 Flames as amplifiers of fluid mechanical disturbances. *Proc. Sixth Natl Congr. Appl. Mech. Cambridge, Mass.* pp. 11–33.

Matalon, M. & Matkowsky, B. J. 1982 Flames as gasdynamic discontinuities. *J. Fluid Mech.* **124**, 239–259.

Matkowsky, B. J. & Sivashinsky, G. I. 1979 An asymptotic derivation of two models in flame theory associated with the constant density approximation. *SIAM J. Appl. Maths* **37**, 686–699.

Pelce, P. & Clavin, P. 1982 Influence of hydrodynamics and diffusion upon the stability limits of laminar premixed flames. *J. Fluid Mech.* **124**, 219–237.

Pelce, P. & Rochwerger 1992 Vibratory instability of cellular flames propagating in tubes. *J. Fluid Mech.* **239**, 293–307.

Peters, N. & Ludford, G. S. S. 1984 The effect of pressure variations on premixed flames. *Combust. Sci. Technol.* **34**, 331–344.

Poinsot, T. J., Trouve, A. C., Veynante, D. P., Candel, S. M. & Esposito, E. J. 1987 Vortex-driven acoustically coupled combustion instabilities. *J. Fluid Mech.* **177**, 265–292.

Schadow, K. C. & Gutmark, E. 1992 Combustion instability related to vortex shedding in dump combustors and their passive control. *Prog. Energy Combust. Sci.* **18**, 117–132.

Searby, G. 1992 Acoustic instability in premixed flames. *Combust. Sci. Technol.* **81**, 221–231.

Searby, G. & Clavin, P. 1986 Weakly turbulent, wrinkled flames in premixed gases. *Combust. Sci. Technol.* **46**, 167–193.

Searby, G. & Rochwerger, D. 1991 A parametric acoustic instability in premixed flames. *J. Fluid Mech.* **231**, 529–543.

Stuart, J. T. 1960 On the nonlinear mechanisms of wave disturbances in stable and unstable parallel flows. Part 1. The basic behaviour in plane Poisuille flow. *J. Fluid Mech.* **9**, 353–370.

Williams, F. A. 1970 An approach to turbulent flame theory. *J. Fluid Mech.* **40**, 401–421.

Williams, F. A. 1985 *Combustion Theory*. Benjamin Cummings, Redwood City.

Yu, K. H., Trouve, A. & Daily, J. W. 1991 Low-frequency pressure oscillations in a model ramjet combustor. *J. Fluid Mech.* **232**, 47–72.